Reactive Oxygen Species Generating Systems Meeting Challenges of Photodynamic Cancer Therapy

Zijian Zhou[a,b], **Jibin Song**[b], **Liming Nie**[*,a], and **Xiaoyuan Chen**[*,b]

[a]Center for Molecular Imaging and Translational Medicine, State Key Laboratory of Molecular Vaccinology and Molecular Diagnostics, School of Public Health, Xiamen University, Xiamen 361102, China

[b]Laboratory of Molecular Imaging and Nanomedicine, National Institute of Biomedical Imaging and Bioengineering, National Institutes of Health, Bethesda, MD 20892, USA

Abstract

Reactive oxygen species (ROS)-mediated mechanism is the major cause underlying the efficacy of photodynamic therapy (PDT). The PDT procedure is based on the cascade of synergistic effects between light, photosensitizer (PS) and oxygen, which greatly favor the spatiotemporal control of the treatment. This procedure has also evoked several unresolved challenges at different levels including (i) limited penetration depth of light restricts traditional PDT to only superficial tumours; (ii) oxygen reliance deprives PDT treatment of hypoxic tumours; (iii) light could complicate the phototherapeutic outcomes due to the concurrent heat generation; (iv) specific delivery of PSs to sub-cellular organelles for exerting effective toxicity remains an issue; and (v) side effects by undesirable white-light activation and self-catalysation of traditional PSs. Recent advances in nanotechnology and nanomedicine have provided new opportunities to develop ROS-generating systems through photodynamic or non-photodynamic procedures while tackling the challenges of current PDT approaches. In this review, we summarize the current status and discuss the possible opportunities of ROS generation for cancer therapy. We hope this review will spur pre-clinical research and clinical practice for ROS-mediated tumour treatment.

Graphical abstract
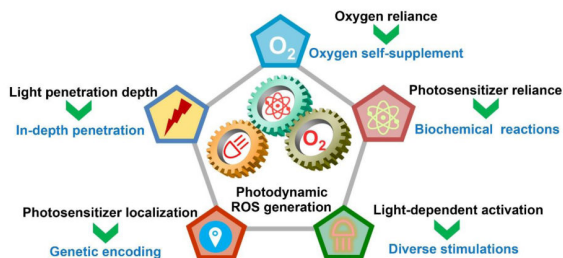
Summary of advanced strategies to generate reactive oxygen species (ROS) through both photodynamic and non-photodynamic procedures for cancer therapy.

[*]nielm@xmu.edu.cn; shawn.chen@nih.gov.

1. Introduction

Reactive oxygen species (ROS) are chemically reactive radicals or non-radical molecules derived from molecular oxygen (O_2), including singlet oxygen ($^1O_2$), peroxide (O_2), superoxide ($O_2\bullet$), and hydroxyl radical (HO$\bullet$).[1, 2] Since the introduction of O_2 into our atmosphere by photosynthetic organisms early in the blossomy evolution of aerobic life, ROS has become an integral part of our earth life.[3] Molecular oxygen has two unpaired electrons with parallel spins located in two separate orbits of its outer electron shell, which makes it highly susceptible to radical formation. The formation of ROS as a byproduct during the photosynthesis and aerobic respiration of plants and other living organisms constantly occurs in chloroplasts, mitochondria, peroxisomes, and cytosol of cells.[4, 5] In mammalian cells, ROS is mainly generated in mitochondria when oxygen is reduced along the electron transport chain during aerobic respiration or by oxidoreductase enzymes and metal-catalyzed oxidation throughout the lifetime of cell cycle.[6]

ROS functions as a double-edged sword in cells.[7] Low levels of ROS play important roles in supporting cellular life cycles, such as proliferation and homeostasis.[8] They act as cellular signaling messengers by reversibly oxidizing protein thiol groups, thereby modifying protein structure and function.[7] More importantly, ROS generation has long been recognized as one of the key factors that protect our body from invading organisms in disease-resistance, cell-mediated immunity, and microbiocidal activity.[9] Cells have a variety of defensive mechanisms to regulate the balance between the formation and elimination of ROS, and thus controlling ROS at a moderate level for normal cellular functioning. However, the imbalance between ROS generation and detoxification could generate oxidative stress with high levels of ROS in the cell. This would result in oxidative damage to cellular constituents (e.g., proteins, lipids, and DNA), apoptosis or necrosis, and probably the promotion of cancer-causing mutations.[10-12] The level of ROS can also indicate different cellular activities that vary in nature and over time. Mounting evidence suggests that many types of cancer cells have increased levels of ROS compared with their normal counterparts.[13-15] Concomitantly, cancer cells have altered redox status by increasing the expression of endogenous antioxidants, which significantly affect the phenotypic behavior of cancer cells and their response to therapeutic interventions.[16, 17] Many cancer cells are thus well adapted to oxidative stress because of their inherently flexible redox status, which makes malignant cells more resistant to exogenous stress, such as chemotherapy and radiotherapy.[18-20]

Modulating the exceptional redox regulatory mechanisms of cancer cells has long been recognized as an effective strategy to eradicate these cells.[21] Many compounds, such as paclitaxel, doxorubicin, arsenic oxide and platinum-based drugs, would promote the generation of cellular endogenous ROS when they exert anticancer activity both *in vitro* and *in vivo*.[22, 23] However, the underlying mechanism for the generation of cellular ROS by these compounds is still unclear. Similarly, the low clinical response and high frequency of drug resistance to these chemotherapeutic agents are also not fully understood.[24, 25] Furthermore, some cancer cells, especially those in advanced stages, are highly adaptive to oxidative stress by upregulating the expression of antioxidants (e.g., glutathione or catalase) which enables them to survive harsher drug treatments. Exploiting the vulnerability of cancer cells to exogenous ROS generation has shown great promise in cancer drug

discovery.[26] In fact, cancer cells have the ability for elevated ROS generation which results in an upregulation of antioxidant(s) and a shift of redox dynamics to maintain the ROS levels below the toxic threshold.[26] It is conceivable that cancer cells would be more dependent on antioxidants for cell survival and thus, more vulnerable to exogenous ROS or on compounds that abrogate the antioxidant systems.[26] This concept of inducing preferential cancer cell death was proposed two decades ago, suggesting that ROS-mediated cancer cell killing strategies may cause more damage to malignant cells than normal cells due to the different redox states.[27-30] It is worth noting that redox alteration in cancer cells is a complicated, multifactorial process and therefore simply introducing ROS-generating agents into cells may not always lead to a preferential killing of cancer cells.[26, 29]

Photodynamic therapy (PDT) is a treatment that employs exogenously produced ROS to kill cancer cells generated from photosensitizers (PSs) or photosensitizing agents by light activation.[31-33] First introduced in the early 1890s and rediscovered in 1975,[34] PDT has been extensively exploited as a promising strategy for cancer cell killing and tumour ablation over the past four decades.[35-37] There are typically three major components involved in PDT: a specific light source that provides energy for a specific type of photodynamic reaction; PSs that can harvest this light and conduct photodynamic reaction; and oxygen-containing substrates (e.g., molecular oxygen, water) that produce ROS upon electron transfer from excited PSs.[36] Since the approval of the first PDT drug procarbazine in 1970s, more than 16 drugs have been developed till now that are commercially available or under clinical trials.[31] Nevertheless, conventional PDT faces several challenges including light penetrating depth, PS and O_2 reliance, PS localization, and light-dependent activation (**Fig. 1**).

Recent advances in nanotechnology have provided a versatile platform for PDT developments.[38, 39] A number of comprehensive reviews have been contributed to elucidate the theory behind the PDT procedure,[40, 41] summarize the judicious optimization of PSs and design of nanostructures for PDT study,[42-44] or underscore the clinical practice of PDT treatment.[31, 37, 45, 46] On this basis, this review is devoted to the innovative systems that aim to produce ROS for cancer therapy and expand the scope of PDT in cancer treatment (**Fig. 1**). We have attempted to provide an overview of such systems by highlighting the critical needs for new PDT treatment strategies while emphasizing the efforts to produce ROS for cancer therapy.

2. Depth penetration

Light penetration depth into the skin is one of the preconditions for a PDT procedure. As a type of electromagnetic radiation, light travels at a particular wavelength and carries a consecutive flow of energy. The entire range of light is divided into several categories as wavelengths increase from 10^{-16} to 10^8 m, including gamma rays, X-rays, ultraviolet (UV), visible light, infrared, and radio waves. Utilizing light as an energy source, photosensitization is an electron transfer (not energy transfer) process from an excited light-absorbing sensitizer to non-absorbing substrate. The penetration depth and delivery efficiency of light are two major obstacles in PDT of cancers for deep tissue treatment, because light can be largely reflected and decayed upon interacting with tissues (e.g., skin).

A similar concern is also valid in photothermal therapy (PTT) that employs light-absorbing agents to generate heat for thermal killing of cancer cells.[38]

The living tissues are a highly complicated dynamic turbid medium which can confer a dominant effect to light by varying the rates of absorption, scattering, transmission and reflection (**Fig. 2**).[31, 47, 48] Penetration depth of light in living tissues depends on multiple parameters such as wavelength, intensity, polarization, coherence, and the tissue physiology, like pigmentation, fibrotic structure, hydration and composition (e.g., hair). Endogenous fluorophores, including hemoglobin and melanin, have strong absorption of light in the visible spectrum below 600-700 nm. Therefore, an ideal PS should have an absorption peak above 700 nm to allow tissue penetration as deep as possible.[49] By taking into account the energy shrinkage with wavelength increment, only the light in the range of 700 and 1100 nm (i.e., near-infrared, NIR) is suitable to penetrate deep into tissue.[50] However, long wavelength NIR light (e.g., >850 nm) was found to be less effective in activating PSs in practical PDT due to the narrow energy gap and the relatively fast non-radiative transition (e.g., thermal effect).[40, 51] Taken together, most of the current PSs have limitations with the wavelength ranging from 700 to 850 nm.[51] In a typical setting, the light penetration depth was reported to be ~3 mm underneath the skin, which largely hinders their wide applications in the clinic.[52]

To overcome the drawback of limited penetration depth in traditional PDT systems, several strategies have been applied. First, one can use light transducers as energy amplifiers that can absorb light in the NIR region and emit in the visible region thereby activating PSs in the vicinity.[53, 54] Such examples can be found in upconversion nanoparticles (UCNPs) and two-photon excited NPs.[55-60] Second, bioluminescence resonance energy transfer (BRET) systems combining bioluminescent luciferase and quantum dots (QDs) could allow *in situ* production of light and internal activation of the PSs due to the unique optical properties of QDs.[61] Third, X-ray as a light source has great promise in PDT applications with no tissue penetrating limitation. This strategy employs nanoscintillators to convert X-ray into visible light and in turn activates the nearby PSs.[62] Fourth, high-speed charged particles, such as positrons (β^+) or electrons, may emit light in the visible spectrum (250-600 nm) when they travel in a given medium faster than the speed of light. This procedure is known as Cerenkov radiation being great potential for depth-independent PDT.[62]

2.1 Upconversion systems

The concept of upconversion is an important photonic phenomenon in photo-physics and chemistry, which describes the conversion of a lower energy excitation into a higher energy emission through an anti-Stokes photoluminescence process.[57, 63] With the emergence of nanotechnology and nanomedicine, UCNPs have attracted tremendous research interest in the fields of materials, energy, bioimaging, and biomedicine.[56, 58-60, 64, 65] Although molecular upconverting systems usually show relatively higher upconversion conversion efficiency than UCNPs, they are still limited in practical PDT study partially due to the challenges to reach favorable NIR excitable range.[66] Recent advances in synthetic and theoretical approaches may open up new avenues to solve these problems by using upconverting molecules for PDT study.[67, 68] The upconverting range of UCNPs can be

easily modulated from NIR to shorter NIR, NIR to visible, or NIR to ultraviolet (UV) emission through engineering the synthetic methods, either by dopant control or by formation of core-shell structure. Moreover, light emitted by UCNPs is considered to be nonblinking and nonbleaching, less light scattering, and capable of deep tissue penetration because the excitation in the NIR region is within the optical 'transparency' window of biological tissues. Therefore, UCNPs have great potential to endure the limitations of light penetration depth in traditional PDT procedure, which serves as a light transducer to emit shorter wavelength light for activating PSs upon NIR light excitation (**Fig. 3A**). There are several strategies to construct PDT formulations based on UCNPs and PSs. First, PSs can be covalently conjugated onto UCNPs through surface functionalization and chemical binding procedures (**Fig. 3B**). Second, PSs can be non-covalently attached to the surface of UCNPs through either hydrophobic-hydrophobic interaction or electrostatic interaction (**Fig. 3C**). Third, PSs can be embedded into mesoporous silica matrix during the formation of UCNP-silica core-shell structure (**Fig. 3D**). Fourth, nanostructured TiO_2 can serve as PS layer coated onto the surface of UCNP as core-shell structure without adding molecular PS (**Fig. 3E**).

Covalent chemical conjugation of PSs onto the surface of UCNPs is quite straightforward; however, this method requires the PSs to be sufficiently hydrophilic to render the overall formulation water-soluble and biocompatible. Unfortunately, most of the current PSs are hydrophobic which limits this method to very few choices of hydrophilic PSs.[69-72] Alternatively, a smartly engineered configuration of 5-aminolevulinic acid (ALA)-conjugated UCNPs have been recently reported as a novel PDT formulation.[73] ALA is an FDA-approved PDT prodrug that can be converted to PS protoporphyrin IX (PpIX) via the heme biosynthesis pathway.[74, 75] In contrast to the directly administered FDA-approved PS Photofrin,[76] ALA molecule is economic, hydrophilic, and more importantly, of higher selectivity in cancerous cells due to the downregulated ferrochelatase (a PpIX degrading factor).[74, 75] When conjugated to UCNPs with high absolute upconversion quantum yield of 3.2% in red-emission, Han et al. demonstrated a significant PDT effect in a deep-seated tumour at a safe laser power density.[73] The covalent chemical conjugation avoids the unexpected release of PS from the UCNPs during systemic circulation. However, covalent conjugation of PS is often associated with low loading efficiency, which is mitigated with the combination of other loading methods to achieve sufficient ROS generation for cancer cell killing.[77]

Delivery of hydrophobic drugs largely relies on the non-covalent physical adsorption or electrostatic interaction methods. The same design considerations were applied to load PSs for constructing light activated PDT platforms.[78] Specifically, the as-prepared UCNPs are usually capped with oleic acid to make the host NPs soluble only in a non-polar organic solvent. For example, Liu et al. reported that Chlorin e6 (Ce6) could be loaded in the tangling framework of hydrophobic alkyl chains by using amphiphilic C_{18}MPH-PEG molecules.[79] The resulting UCNP-Ce6 supramolecular complex showed excellent PDT efficacy and tumour suppression.[79] The authors further demonstrated that $^1O_2$ generation maintained at the level of 50% when a piece of 8 mm thick pork tissue was placed under the 980 nm laser, while no $^1O_2$ was detected when excited at 660 nm. On the other hand, Chen

et al. reported that the exposed positively charged Ln^{3+} ions on the surface of UCNPs can be attached with negatively charged mono-substituted β-carboxyphthalocyanine zinc (ZnPC-COOH) molecules, resulting in a high energy transfer efficiency of 96.3% (the highest value reported to date).[80] Non-covalent loading of PSs allows for close interaction with the UCNPs, which in turn confers high energy transfer efficiency for effective ROS generation. Moreover, other hydrophobic drugs (e.g., chemotherapeutic drugs) can be combined with PSs using this method, which would further enhance the tumor-killing effect.

Surface coating of a silica layer was widely employed to incorporate PSs with UCNPs, which are usually embedded into the mesoporous silica shell.[81-84] The unique porous structure of mesoporous silica layer facilitates diffusion of oxygen species (e.g., H_2O or O_2) into the channels and interaction with the loaded PSs.[85] This method has several advantages: (i) both hydrophobic and hydrophilic PSs can be loaded into the porous silica layer; (ii) the size of mesoporous channels can be easily tuned to modulate the loading efficiency and interacting profile of different PSs with different molecular sizes; (iii) positively charged PSs are especially suitable for this system due to the negatively charged nature of the silica matrix. It is noteworthy that this method is a slow multistep process and the PS loading efficiency is highly variable from batch to batch.[39]

Integration of UCNPs with molecular PSs has shown great promise in ROS generation at the deep tissue level. However, molecular PSs often suffer from uncontrollable loading and leakage due to the highly diffusive nature even when incorporated into nanoparticles; this also attenuated the reliability and reproducibility of PDT results both *in vitro* and *in vivo*. TiO_2 nanoparticles are excellent regenerative photocatalysts that can absorb ultraviolet light at a range of 275 to 390 nm and generate cytotoxic ROS with high efficiency.[86] ROS can be produced through electron-hole transfer from TiO_2 nanoparticles to either chemisorbed water in an oxygen-independent manner or molecular oxygen in aerobic conditions.[87, 88] Recently, Zhang and co-workers reported that UCNPs coated with a layer of TiO_2 shell had highly stable ROS generation without the use of molecular PSs.[89, 90] This design eliminates the possibility of PSs leakage, thus ensuring significant and stable ROS outputs for efficient killing of cancer cells.[90]

2.2 Two-photon excitation

As a nonlinear optical phenomenon, two-photon absorption (TPA) is the simultaneous absorption of two photons of identical or different frequencies to excite the ground state of molecules to an excited higher energy state. This approach has attracted increasing interest in recent years.[91] The TPA protocol requires the use of a tightly focused femtosecond laser beam as a light source to excite a small focused area and obtain sufficient instant energy for two-photon excitation.[56] In contrast to other upconverting processes in which photon adsorption could happen non-synchronously, TPA occurs only when two photons are simultaneously absorbed. The light intensity is maximized at the focal plane and decreases approximately with the square of the distance along the propagation direction. Thus, excitation through TPA is confined in a small area near focal plane, giving the extraordinary opportunity to pinpoint 3D images with high spatial selectivity.[91, 92]

Therefore, two-photon-excited PDT is a promising strategy for deep-tissue penetration and selective activation of PSs by using femtosecond pulsed NIR laser (**Fig. 4A**).[93-95] A proof-of-concept *in vivo* study for two-photon PDT was reported in 2008 by Wilson and Anderson groups, who developed a new family of porphyrin-based PSs with high two-photon cross-sections (**Fig. 4B**).[96] The authors demonstrated that the TPA cross-sections of these porphyrin dimers were more than two orders of magnitude greater than those of standard clinical PSs, remarkably facilitating the TPA process (**Fig. 4C, D**). The use of NIR laser light (920 nm, 300 fs, 90 MHz, 39 mW) efficiently activated the PSs for ROS generation and cell death (**Fig. 4E**). The selective occlusion of mouse artery with a diameter of about 40 mm at the focal point of the laser was observed while leaving the surrounding tissue unaffected.[96]

Starkey et al. reported the development of an MPA79-based derivative with the corresponding maximum TPA cross-section of 1500 to 2000 Goeppert-Mayer units.[95] This molecule allowed for robust regression of tumour xenografts at the depth of 2 cm through the body of severe combined immunodeficiency (SCID) mice by two-photon PDT. The results further indicated the high potential to lay a maximum depth at 5 to 7 cm in larger animals. Intelligent artificial synthesis and modification of porphyrin-based molecules for enhanced TPA have been extensively explored.[97-100] Kobuke and co-workers reported that the butadiyne-linked bisporphyrin array system showed strongly enhanced TPA exhibiting a potential for an enhanced energy transfer and PDT efficacy upon two-photon activation.[97, 101] Despite the extensive research interest, these molecular TPA materials often suffer from severely decreased quantum yield after transferring into water through molecular engineering or nanoparticle formulation.[102]

Jiang and colleagues reported a considerable large increase in the quantum yield of CdSeS/ZnS QDs from 0.33 to 0.84 after polymer encapsulation, probably due to the blocking of non-radiative decay pathway from the surface trap states of QDs.[102] The resultant QDs exhibited a notable penetration depth of 2.2 cm in two-photon imaging of cells underneath a tissue phantom, suggesting the feasibility of utilizing QDs as two-photon mediated deep tissue PDT probes. Plasmonic metal NPs (e.g., Au, Ag) are known to have unique optical properties arising from collective oscillation of conduction band electrons on surfaces, which can induce local electromagnetic fields and modulate optical properties of nearby chromophores. Furthermore, Au nanostructures were reported to possess about two orders of magnitude higher TPA cross-sections than those of traditional fluorophores, making them attractive candidates as TPA probes and light transducers in PDT.[103, 104] Recently, a FRET system based on two-photon excited silica-coated gold nanorods (GNRs) and PSs has been investigated by adjusting the thickness and porous feature of silica shell between the donor and acceptor.[105, 106] The optimal two-photon energy transfer was achieved with the silica thickness of 20 nm which caused severe damage to epithelial tumour model by TPA-PDT procedures.[105]

2.3 Self-illumination

Analogous to FRET, BRET utilizes biochemical stimulus to activate bioluminescent proteins which in turn serve as donors to excite acceptors (e.g., fluorophores or proteins) in close

proximity.[107, 108] First discovered in marine creatures such as jellyfish *Aequorea Victoria* and the sea pansy *Renilla reniformis*, BRET has additional advantages over FRET because the emission and the activation in BRET can be remotely controlled through biochemical reactions. These features provide invaluable opportunities for *in vivo* imaging and biosensing. The enzyme Renilla luciferase (Rluc) and its substrate coelenterazine are one of the most widely used donor counterparts in artificial BRET platforms.[109] Rluc catalyzes the oxidation of coelenterazine, which is a cell-permeable molecule, and emits light at the maximal wavelength of 480 nm depending on the structural nature of the substrate.[110, 111] The unique optical properties of QDs, especially for the large Stokes shift, make them appealing as leading candidates in BRET system where locally excited weak bioluminescence can be converted into bright fluorescence at a longer wavelength.[112] Therefore, locally activated BRET systems are amenable for deep tissue bioimaging and sensing which could overcome the shallow tissue penetration of light in traditional light-dependent platforms.[61, 113]

Recently, a BRET system by Rluc illuminating QDs has been demonstrated for deep tissue PDT.[114, 115] Dated back to 1994, a similar concept of bioluminescence-based PDT was reported by Carpenter et al., who investigated its potential using Photinus pyralis luciferin/ luciferase system as bioluminescence light source.[116][117, 118] Rao et al. developed an eight-mutation variant of Rluc, denoted as Rluc8, which is more stable in serum and has improved catalytic efficiency compared with the wild-type protein, suitable for BRET imaging and bio-sensing *in vivo*.[61]

A BRET-mediated PDT system was reported by Lai and co-workers in which Rluc8 was immobilized on the surface of CdSe/ZnS QDs which showed a cascade of BRET and ROS generation after adding coelenterazine (**Fig. 5**).[114] BRET excites fluorescence emission of QDs at 655 nm which in turn activates the PSs (Foscan) in close proximity. The generation of ROS was calculated to be ~40.8%, killing A549 cells *in vitro* and significantly delaying tumour growth *in vivo*. Yun and colleagues further reported that Rluc8-decorated QDs showed efficient BRET-induced PDT for the treatment of macroscopic tumours and metastases at sentinel and secondary lymph nodes (LNs) in deep regions.[115] The authors demonstrated that not only the primary tumour but also the metastatic cancer cells in inguinal LNs were significantly reduced in the treated group, highlighting the great potential for BRET-mediated PDT of tumours located in deep tissues which cannot be reached by external optical illumination.[115]

2.4 X-ray excitation

X-rays are a part of the electromagnetic spectrum with frequencies in the range of 3×10^{16} to 3×10^{19} Hz and energies in the range of 0.1 to 100 keV. Different from traditional light, X-rays can ionize atoms and disrupt chemical bonds of molecules due to the high-carrying energy. In terms of energy, X-rays are categorized into 'hard' and 'soft' X-rays with energies above 5-10 or less than 5 keV, respectively. Despite considerable risks of radiation sickness and cancer-causing potential, X-rays have been widely applied in medical imaging due to their considerable merits in disease examination.[62]

X-rays interact with matters by three major mechanisms of photoelectric absorption, Compton scattering, and pair production. It is of note that the interaction is scantly related to chemical properties because X-ray photon energy is much higher than chemical binding energies of applied materials. For medical imaging of organisms by hard X-rays, photoelectric absorption is the major interaction between X-rays and bone structures which make them clearly show up in images due to the presence of calcium, while Compton scattering is the dominant interaction between X-rays and soft tissues. In other words, heavy metals can enhance the ionizing effects of X-rays through the "high-Z effect", exhibiting higher photoelectric cross sections than soft tissues using sub-mega-electronvolt energies.[62, 119, 120] The employment of high-Z substances (usually containing heavy metals) to generate X-ray-excited optical luminescence (XEOL) has been a promising technology for molecular imaging and biomedical applications.[121, 122]

X-ray photons hold great potential to serve as an ideal excitation source, enabling penetration into deep tissues.[62, 123] To this end, X-ray-excited PDT procedure could be highly potent in overcoming the limitation of light penetration depth in traditional light-activated PDT. In this process, wide band gap materials are employed as scintillators to absorb incoming X-rays and transform them into UV/visible light. This phenomenon is attributed to the interaction between high energy photons and scintillators through photoelectric effect and Compton scattering effects (**Fig. 6A**). Recently, several types of nanoparticles have been developed for this purpose, such as metal-organic frameworks,[124] gold nanoclusters,[125] radioluminescent nanophosphors,[126, 127] QDs,[128] and lanthanide-based NPs.[129, 130] The emission of UV/visible light can be subsequently harvested by nearby PSs to generate ROS (**Fig. 6B**). Also, the use of X-rays enables super-high penetrating depth and excitation of locally loaded PSs when they are in deep-seated tumours.

A pilot study performed by Chen et al. demonstrated that X-rays can activate Ce^{3+}-doped lanthanum(III) fluoride ($LaF_3:Ce^{3+}$) or ZnS:Cu,Co particles to emit scintillation or persistent luminescence, which in turn activates the PSs to generate $^1O_2$ for cancer cell destruction.[131, 132] The authors showed that this strategy was able to effectively kill cancer cells *in vitro* upon a 5 Gy X-ray irradiation, holding great promise for deep seated cancer treatment.[123, 133] Xie group developed a novel $SrAl_2O_4:Eu^{2+}$ (SAO) NPs as an X-ray inducible nanoscintillator, which induced substantial tumour growth arrest and even tumour shrinkage in a U87MG xenograft model.[127] More recently, Shi group developed a core-shell Ce(III)-doped $LiYF_4@SiO_2@ZnO$ structure to combine synchronous radiotherapy and ionizing radiation-induced deep PDT (**Fig. 6C-F**).[134] The radiation-induced PDT demonstrated substantially enhanced antitumour therapeutic efficacy with minimal dependence on the light penetration depth and oxygen levels in mouse tumour models (**Fig. 6G, H**).[134]

The feasibility of using high-energy photons (e.g., X-ray, γ-ray) as light sources for PDT has recently been quantified in a model of CeF_3-verteporfin (VP) conjugates.[135] The results showed that the quantum yield of X-ray induced $^1O_2$ generation was 0.79 ± 0.05 for the most efficient conjugate with 31 VP molecules per nanoparticle. This conjugate converts $^1O_2$ molecules at the level of 1.2×10^8 to 2.0×10^9 per cell upon exposure to high energy (6 MeV) radiation with a radiotherapeutic dose of 60 Gy. Furthermore, another study

employed Monte Carlo program to model energy deposition and predicted the efficiency of nanoscintillators in X-ray-induced $^1O_2$ generation, emphasizing several key factors that would balance the PDT effect, such as coupled PSs, X-ray energies, NP concentrations, and NP sizes.[136]

2.5 Cerenkov radiation

Cerenkov radiation, named after Pavel Alekseyevich Cerenkov, is an electromagnetic radiation when a charged particle (β- or α-particle) travel through a dielectric medium at a speed faster than light.[137] As a charged particle, it can polarize the molecules of its medium into an excited high-energy state. One of the most important characteristics for Cerenkov radiation is the emission of Cerenkov luminescence (CL), which is generated from the process of polarized molecules relaxing back to the ground state.[137] The emitted radiation luminescence consists of light within continuous spectrum (ca. 200-1000 nm) with a broad energy range (ca. 6.1-1.23 eV). The CL-based strategies have recently attracted attention in molecular imaging applications and serve as an effective tool to bridge the radionuclide imaging with optical imaging.[138, 139] For example, Moore and colleagues reported a proof-of-concept study that 2-deoxy-2-[^{18}F]fluoro-D-glucose (^{18}FDG) could be used as PET-activated probe in a luciferase-transfected breast cancer model.[140]

Similar to X-ray-induced PDT process, high energy positron (β^+) internalized Cerenkov radiation, with greatly enhanced tissue penetration depth, can also be utilized in phototherapeutic studies. However, CL is still a low-intensity light source because of the low Cerenkov photon flux from the radiotracers. Significant signal amplification and optimized light-harvesting procedures are therefore required to exert efficient Cerenkov-radiation-mediated therapy.[137] TiO_2 nanoparticles are excellent regenerative photocatalysts that absorb ultraviolet light (λ = 275-390 nm) with high efficiency to generate cytotoxic ROS (e.g., $O_2\bullet^-$ and HO•).[86] The HO• are produced through electron-hole transfer to H_2O molecules adsorbed on the surface of TiO_2 nanoparticles in an oxygen-independent process This approach holds great potential to induce toxicity to hypoxic tumours.[87, 88] Achilefu et al. have explored the use of TiO_2 nanoparticles as PSs for CR-induced phototherapy (CRIT, **Fig. 7A**).[141] The authors employed apo-transferrin (Tf) as a tumour-targeting agent coated onto TiO_2 nanoparticles, providing a modular approach for PSs design and an efficient tumour-targetable CRIT (**Fig. 7B, C**).[141] The results showed that CRIT is effective only when both the CR source (^{18}F and ^{64}Cu) and the PSs are in the same cell, while maintaining off-target toxicity at a low level. Finally, an *in vivo* study employing the intravenous administration of tumour-targeting NPs showed that CRIT significantly inhibited the growth of the A549 tumour (**Fig. 7D-F**).[141]

Although the use of radioisotopes as a light source can greatly alter the limited penetration depth of an outside light source, Cerenkov radiation is still restricted by its effectiveness. First, the luminescence intensity from Cerenkov radiation is several orders of magnitude weaker than that of conventional fluorescence imaging, because most of the radiated energy is in γ-photons rather than β-particles. Second, Cerenkov radiation is mainly composed of UV-blue photons which have limited tissue penetration depth. The combination of CR and energy transfer mediators to improve CL intensity is considered as a promising strategy to

achieve enhanced PDT outcomes, such as the use of QDs,[138] gold[142] or europium oxide[143] nanoparticles.

3. Oxygen self-supplement

A solid tumour often has fast proliferation exceeding its blood supply due to the imperfect vascular system leaving portions of the tumour in a hypoxic microenvironment.[144, 145] A variety of tumour treatments, such as chemotherapy, radiation and hyperthermia therapy, are ineffective because of the low tumour oxygenation levels.[146, 147] Hypoxic tumour regions may thus be excluded from therapy, resulting in inevitable tumour recurrence and metastasis.[148, 149] Hyperbaric oxygen therapy which entails the use of pressurization to deliver increased oxygen concentration to the body and especially in the tumour has been developed.[147, 150] Since the 1970s, this strategy has been introduced in clinical trials with patients undergoing radiotherapy in hyperbaric oxygen chambers in an attempt to force more oxygen into blood and into the tumours.[150] Indeed, breathing hyperbaric oxygen can increase the pressure of oxygen (pO_2) in tissues of the patient. For example, pO_2 of skin dermis increases from about 50 torr when breathing air (20% oxygen) to 150-350 torr during the breathing of 100% oxygen at 1 atm.[151] This value can be increased to above 1000 torr by breathing of 100% oxygen at 2 to 3 atm.[151] Researchers have also shown that breathing hyperbaric oxygen could increase the ROS levels in patients, implying the critical role of oxygen in disease treatments.[147]

The photodynamic procedure through PSs excitation via the triplet state can be characterized as Type I and Type II processes.[39] Type I reaction comprises the directly activated reactions between PSs and substrate molecules *via* electron or hydrogen atom transfer and usually gives rise to free radicals.[39] In the Type II process, which is dominated by most of the current dye PSs, the electronically excited PSs react with oxygen to form ROS.[39, 62] Therefore, the availability of molecular oxygen may become a rate limiting factor in producing ROS through the Type II process (**Fig. 8**). Previous studies have shown that tumour hypoxic condition could largely abolish PDT-mediated cell inactivation.[152, 153] An *in vitro* study using Photofrin II as PS showed full PDT effects when the pO_2 level was at about 40 torr and half the effects at about 8 torr.[154] It has also been reported that oxygen level dramatically decreases during and after photodynamic treatment, largely attenuating the effectiveness of ROS production and PDT outcomes.[155] Under more severe conditions, PDT could shut down the tumour vasculatures during ROS production depriving the tumour of oxygen and suspending the photodynamic process.[156] Studies have shown that the combined hyperbaric oxygen therapy and PDT may enhance the effectiveness of PDT compared with PDT alone.[46, 150] Although PS dosage and light dosimetry have been well standardized in PDT procedures, the oxygen level and the hypoxic microenvironment within tumours cannot be controlled, leading to ambiguous outcomes in a number of PDT studies.

To enhance the availability of oxygen in the tumour during PDT treatment, several strategies have been developed including hyperbaric oxygen enrichment, prevention of vascular shutdown, and *in situ* oxygen self-supplement. Although the hyperbaric oxygen treatment can enhance the oxygen level in tumour plasma, the practical feasibility of hyperbaric-mediated PDT seems to be limited.[147] Modulation of other parameters, such as the light

exposure cycle, may be more easily achievable in terms of efficacy. The prevention of vascular shutdown is executable by pre-administration of heparin, a clinically used drug for preventing thrombosis and disseminated intravascular coagulation.[157] This strategy could temporarily reduce thrombosis in tumour region during light irradiation, showing enhanced therapeutic effect in an EMT6 mammary carcinoma model.[157] Since the first two methods are beyond the scope of this review, we mainly highlight the oxygen self-supply systems enabling the on-demand production of molecular oxygen to promote PDT treatment (**Fig. 8**).

3.1 Artificial red blood cells

Red blood cells (RBCs) are known as essential vehicles to transport oxygen (as well as carbon dioxide) through the blood stream of all vertebrates.[158] Hemoglobin (Hb) is the iron-containing metalloprotein inside RBCs that carries oxygen from the lung and returns carbon dioxide to lung during respiration.[158] Each Hb molecule contains four heme groups to which oxygen can bind. However, bare Hb itself is not suitable for oxygen delivery due to the short circulation half-life and poor stability which requires adequate decorating techniques to 'mask' them into composites denoted as artificial red cells (ARCs).[159, 160] With the emergence of nanotechnology, various approaches have been engineered for this purpose.[160, 161] In this respect, the ARCs internalized PDT systems may have the potential to boost photodynamic efficacy.

Wang's group reported a hemoglobin (Hb)-based oxygen carrier that was chemically conjugated to a tri-block copolymer.[162] The self-assembly of copolymers led to the formation of micelles encapsulated with a second-generation PS zinc phthalocyanine (ZnPc). The Hb was evaluated after conjugation for oxygen-binding capacity and antioxidative activity, which would compensate the oxygen demands during ROS production. Importantly, the resulting PDT formula was able to generate more $^1O_2$ and greater photocytotoxicity in Hela cells *in vitro*, compared to ZnPc-loaded micelles without Hb.[162]

Cai et al. developed a biomimetic lipid-polymer as ARC containing Hb as an oxygen carrier and indocyanine green (ICG) as PS.[163] The ICG was incorporated with the subunits of Hb at the interface through extensive electrostatic and hydrophobic interactions (**Fig. 9A-C**). The proximal distance between ICG and heme enables self-supplied oxygen molecules for efficient ROS generation during the PDT procedure. The oxidation of ambient ferrous-Hb to cytotoxic ferryl-Hb species by ROS has shown synergistic effects on cancer destruction (**Fig. 9D-H**). Overall, such an ARC system provides an effective way to replenish oxygen consumption during PDT treatment, which holds great potential for suppression of hypoxic tumours.[163, 164] More recently, Xie's group reported ferritin modified RBCs as an oxygen self-supplied PDT formulation, which showed effective tumour suppression in a subcutaneous U87MG tumour model.[165]

3.2 Perfluorocarbon nanoparticles

Perfluorocarbon molecules are a series of fluorochemicals with the formula of C_xF_y, which are derivatives of hydrocarbons by replacing all the C-H bonds with C-F bonds.[166] Due to the low surface tension, viscosity, and chemical inertness in biological systems,

perfluorocarbons have been widely used in both industrial and medical applications, such as cryogen, anesthesia, radiotherapy regulation, and vitreoretinal surgery.[167-169] Several perfluorocarbons have been approved by the US Food and Drug Administration (FDA) for contrast-enhanced ultrasound imaging.[170] Contrary to the hemoglobin example, oxygen molecules are internalized into perfluorocarbons through physical force-mediated adsorption. Therefore, the amount of oxygen dissolved in perfluorocarbons increases linearly with oxygen tension and is inversely related to temperature. The solubility of oxygen in perfluorocarbons is approximately 40-50 mL oxygen per 100 mL liquid under 760 torr (1 atm) at 25 °C, making them highly suitable to serve as blood substitutes.[166] This value is more than twofold higher than that of the whole blood with a coefficient of approximately 20 mL oxygen per 100 mL under the same conditions.[166] Researches have also shown that perfluorocarbons can prolong cell survival under hypoxic environment owing to the controlled release of oxygen.[171-173] Therefore, perfluorocarbons are potentially valuable oxygen modulators and should be of great potential to replenish oxygen consumption and promote ROS generation in PDT studies.[174, 175]

The use of perfluorocarbons has been recognized as a useful strategy to improve oxygenation level of solid tumours, and thus increase their vulnerability to therapeutic methods during and after treatments, such as ionizing radiation[134, 169] and chemical drugs.[170, 173, 176, 177] Specifically, oxygen-favoring PDT would deplete oxygenation level through photochemical consumption and occlusion of blood vessels.[146] Therefore, perfluorocarbon-integrated PDT with a continuous supply of molecular oxygen could be an innovative strategy to diminish the oxygen dependence. The *in situ* release of oxygen from securely loaded perfluorocarbons would achieve significantly enhanced PDT outcomes, especially suitable for the treatment of hypoxic tumours.

The perfluorocarbons are usually formulated as an emulsion to improve their aqueous miscibility. Lipid formation through a self-assembly process is one of the most powerful tools in utilizing perfluorocarbons after exposure to a high oxygen tension environment. Recently, Hu and Wu et al. used a perfluorocarbon nanodroplet as a carrier for both PS and oxygen to develop a novel oxygen self-enriched PDT (Oxy-PDT).[178] The near-infrared PSs IR780 were used to impart irradiation by 808-nm laser, which was uniformly dispersed in a lipid monolayer along with perfluorocarbons covered by PEG (MW 2000) on the surface (**Fig. 10A, B**). This system did not rely on the pre-existing hypoxia, oxygen consumption, or vascular damage during PDT treatments and showed a higher therapeutic efficacy of Oxy-PDT than traditional PDT both *in vitro* and *in vivo* (**Fig. 10C-E**). Furthermore, the $^1O_2$ lifetime is considerably much longer in perfluorocarbons than in water, which could lead to long-lasting photodynamic effects (**Fig. 10F, G**). Overall, the self-enriching oxygen offers a simple yet effective solution to the limitation of oxygen reliance in traditional PDT.

Although the use of oxygen-carrying perfluorocarbons seems to be a promising experimental tool, the optimization of systemic administration and elimination of perfluorocarbons should be taken into account. Also, extensive exposure to perfluorocarbons could potentially cause immediate and long-term side effects in some individuals, such as hypotension, cutaneous flushing, fever, pulmonary hypertension, chest tightness, and

elevated central venous pressure.[179, 180] Therefore, clinical translation of perfluorocarbon-integrated PDT should be carefully evaluated.

3.3 Catalase

Catalase is an enzyme that catalyzes the decomposition of H_2O_2 to water and oxygen in aerobic living organisms. The high efficiency of catalase, which converts approximately 5 million H_2O_2 molecules each minute, is invaluable in preventing cellular damage from high levels of H_2O_2 molecules.[181] Inhibition of catalase activity has shown a great impact on cell apoptosis due to the elevation of oxidative stress.[181] The oxygen-evolving photodynamic process requires exogenous delivery of catalase to enhance the phototherapies, since the distribution of catalase in organisms is not precisely known.[182, 183]

To this end, Guo and He et al. recently reported an H_2O_2-activatable O_2-evolving PDT (HAOP) nanoparticle employing catalase to produce oxygen and enhance photodynamic procedure.[184] The catalase molecules were co-loaded with methylene blue (MB) into the aqueous core of poly (D, L-lactic-co-glycolic acid) (PLGA) NPs, where the photodynamic transition was spontaneously quenched by black hole quencher-3 (BHQ-3) at the shell (**Fig. 11A**). Cyclic RGD peptide was decorated on the NP surface to selectively target $\alpha_v\beta_3$ integrin-rich tumour cells. By penetrating H_2O_2 into the PLGA NPs, catalytic production of oxygen could disrupt the PLGA NPs and neutralize the quenching of MB, leading to efficient ROS generation upon laser excitation (**Fig. 11B**). The phototoxicity of HAOP NPs showed prominent therapeutic effects in the U87MG tumour (**Fig. 11C, D**).[184] Another study by Tang's group employed phenyl mesoporous silica-coated Au rods to wrap catalase enzyme onto the surface, which showed similar PDT outcomes.[185] More recently, manganese dioxide (MnO_2) NPs were used in this system, further highlighting the promise of modulating tumour microenvironment to deprive oxygen-dependence from current PDT.[186]

4. Diverse stimulations

Light activation of PSs offers the first level of spatiotemporal control of ROS generation. The judicious use of light has facilitated a great deal of control of ROS production mainly through the photodynamic process. The external light has the merit of on-site stimulation that selectively irradiates the region of interest by photo-toxicity while leaving non-irradiated area unaffected. However, besides tissue penetration limits, light excitation could also have equivocal biological response effects (e. g., heat generation) in cells and tissues, which complicate the phototherapy outcomes. In general, phototherapies are often developed as confluent PTT/PDT systems for synergistic treatment of tumors.[38] Even though significant progress has been made in the intelligent selection of light sources, the available systems are still indiscriminate due to the unavoidable activation of PSs under daylight exposure or by self-catalyzed reactions.[38, 39] To avoid potential side effects, patients during and after administration of PSs are required to stay away from the daylight exposure, which increase the abundant of patients under PDT treatments.[31] The critical design considerations to minimize systemic toxicity during PDT studies are highly desirable.[187]

Recently, the employment of stimuli other than light for ROS generation has received increasing attention (**Fig. 12**). Although light may still be needed, smartly engineered systems that rely on additional controls would confer greatly enhanced safety for ROS-mediated cancer therapy. In this section, we will concisely introduce the examples that were intelligently designed to exhibit responsive ROS production by diverse stimulations.

4.1 Heat

As an easily accessible source of energy, heat has been widely used to activate numerous transformations. Plasmonic nanoparticles (e.g., Au, Ag) have efficient photonic adsorption due to the presence of surface plasmon resonance (SPR) effect.[188-191] Many nanoprobes based on remotely controlled heat generation have been developed for on-demand delivery and release of cargos for biomedical imaging and therapy.[192-194] Based on this rationale, it is worth noting that many $^1O_2$ scavengers can release the $^1O_2$ through a reverse process upon heating.[195, 196] In fact, endoperoxides, such as naphthalene, anthracene, and a few other arenes, are the most reliable chemical sources of $^1O_2$ for studying their chemiluminescence property.[197]

To demonstrate the potential of anticancer effect, Akkaya and Yoon et al. modified gold nanorod (GNR) with anthracene endoperoxide derivatives (EPT1) (**Fig. 13A, B**).[198] Due to the strong plasmonic heating effect of GNRs in the NIR region, Hela cells when incubated with EPT1-GNRs showed prominent oxidative stress and cell death under irradiation with 808 nm NIR laser (2.0 W·cm^{-2}) for 10 min (**Fig. 13C, D**). In contrast to PDT, chemical generation of $^1O_2$ is independent of the external supply of oxygen, which surmounts the hypoxic environment of tumours. In this study, however, a relatively high temperature (~60 °C) was required to release $^1O_2$, which may hinder their wide applications.

Another study has reported a similar concept of storing $^1O_2$ in a bifunctional chromophore to allow the production of $^1O_2$ in a bimodal light/dark circle.[199] By mimicking the fractional PDT for replenishment of intracellular oxygen, a BODIPY-based pyridine compound (PYR) is activated by light irradiation to generate $^1O_2$, some of which would be "stored" in the form of 2-pyridone endoperoxide (EPO). This system benefits from the thermal cycloreversion of EPO to produce $^1O_2$ in the absence of light when irradiation is turned off in fractional PDT. It is worth noting that the cycles between PYR and EPO can be repeated indefinitely. Considering the limitation of light penetration depth into tissues, local thermal cycloreversion enabling continuous production of $^1O_2$ in the dark would be a promising improvement of traditional PDT.[200] Furthermore, these molecules acting as oxygen-independent PSs would partially undermine the intrinsic tumour hypoxia and PDT-induced hypoxia environment.

4.2 Ultrasound

Ultrasound (US) has been widely used as a medical tool both for imaging and therapy.[201] The development of US-based medical practice can be traced as far back as the early 19th century before US imaging was in practice in the 1950s.[202] Among modern clinical settings, the merits of non-ionization and non-radiation make US a powerful mean to visualize organs under the skin, which is especially useful for viewing the fetus during pregnancy. By

modulating the applied ultrasonic power, US can be used as an external energy to exert damages to subjects. Hence, US is probably an alternative choice of energy source to spatiotemporally control the biological effectiveness of applied formulations in a noninvasive manner.[203, 204]

Yeh et al. reported an H_2O_2-filled polymersome displaying echogenic reflectivity and ROS-mediated cancer therapy triggered by a micro-US diagnostic system.[205] The polymersome composed of PLGA polymers was initially encapsulated with H_2O_2 in the hydrophilic core and Fe_3O_4 NPs packed in the shell. Upon exposure to US, the disruption of PLGA polymersome triggered the release of H_2O_2 which subsequently reacted with nearby Fe_3O_4 NPs packed inside the polymersome membrane. The formation of HO• following a Fenton reaction showed prominent cancer cell killing effect. Details of ROS generation by Fenton reaction will be further discussed in Section 6.3. US-triggered ROS generation in this study via a non-thermal and non-photo process is an efficient PS-free therapeutic option to completely suppress tumour growth in a mouse model.[205] Furthermore, US can be utilized as a direct energy source to activate hydrophilized titanium dioxide ($HTiO_2$) NPs and generate ROS with high efficiency (**Fig. 14A-C**).[206] The $HTiO_2$ NPs effectively suppressed the growth of superficial tumours after US treatment with elevated levels of proinflammatory cytokines and intense vascular damages (**Fig. 14D-F**). Another study showed that the combination of light and US activation of PSs generated higher levels of ROS than either one alone.[207]

4.3 Cancer-specific stimulations

To minimize undesired damage to healthy tissues during PDT treatment, one can control the photosensitization of ROS at different levels.[208] These strategies with a broad range of spatiotemporal controls include: (i) precise delivery of external exciting source exclusively to the desired tissue; (ii) active targeting of PSs to targeted foci surpassing healthy tissue;[209-211] and (iii) specific activation of a photosensitizer in the target tissue.[43, 76, 212, 213] Distinctive from the first and the second strategies, the third strategy collaborates with cancer cells themselves to kill them, which could be an ingenious manner to lower the side effects when treating tumours.[76]

During a typical type II photodynamic process, the intersystem crossing from singlet excited state to triplet excited state of PSs is the major mechanism to transfer ground state molecular oxygen ($^3O_2$) to $^1O_2$.[214, 215] This process could be manipulated by introducing a chromophore to quench the photosensitizing effect of PSs nearby, thus attenuating the production of $^1O_2$ species. It is also possible to scavenge $^1O_2$ even after it has been generated. FRET is a non-radiative energy transfer process by which the excited state PS donor can transfer energy to an acceptor that shares absorptive spectral overlap with the PS fluorescence emission. By combining the process of PDT and FRET, an $^1O_2$ quencher/scavenger is thus able to deactivate the photosensitization of proximal PSs.[216] The advantage here is that the FRET will be effective only when the PS and quencher are closely linked in nanometer range through well-designed chemical binding and physical attachment. This type of FRET-based PDT can be explored at a broad scale for materials ranging from molecules and metal-organic-frameworks to nanostructures.[217-219]

The disease-specific segment can be designed to link donor and acceptor which enables to specifically react with an endogenous stimulus existing predominantly in the tumour, such as tumour-specific enzymes, acidic environment, ROS levels, and so on.[76, 220] This method relies on the exploration of the proteomic or metabolic differences between cancer cells and healthy cells, which could be a general solution to achieve cancer-specific inhibition and tumour ablation.

4.3.1 Enzymes—As a proof-of-principle study, Zheng's group reported a protease-activatable Pyro-peptide-CAR (PPC) that consists of a pyropheophorbide *a* (Pyr) as PS and a carotenoid as $^1O_2$ quencher/scavenger linked by a cleavable caspase-3 substrate, GDEVDGSGK.[213] The peptide can be specifically cleaved in the presence of caspase-3, which belongs to the well-known tumour targeting protease family,[221] allowing for restoration of photosensitization and production of $^1O_2$ (**Fig. 15A,B**). The $^1O_2$ quenching and PS-beacon activation were validated by measuring luminescence and lifetime of $^1O_2$ in solution. The PPC was then tested for caspase-3 cleavage using HPLC to monitor the diminishment of PPC peak and the rise of Pyro and CAR residue peaks (**Fig. 15C-F**). The same group further extended the concept of a photodynamic molecular beacon (PMB) to construct a matrix metalloproteinase-7 (MMP7)-triggered $^1O_2$ production system.[212] The PMB was responsive specifically to MMP7, while there was no beacon activation in the presence of an MMP-7 inhibitor. Preliminary *in vitro* and *in vivo* studies in KB cells with high expression of MMP7 also revealed the activatable PDT efficacy, which highlighted the tumor-targetable PDT at the molecular level while precluding healthy cells from $^1O_2$ induced damage.

Choi et al. developed a PS-conjugated GNR (MMP2P-GNR) system in which PSs were conjugated onto the surface of GNR via a protease-cleavable peptide linker.[222] FRET between PSs and GNR efficiently suppressed the fluorescence and phototoxicity of the PSs in their native state. When exposed to target protease matrix metalloprotease-2 (MMP2), the PSs were activated by cleavage of the peptide linker. *In vitro* cell studies in HT1080 cells overexpressing MMP2 indicated efficient fluorescence recovery and $^1O_2$ generation, while the control BT20 cells lacking MMP2 showed minimal effects. The enzymatic cleavage of FRET linkers could be extended to a broad family of enzyme-substrate systems specifically existing in cancer cells.

4.3.2 pH—The increased fermentative metabolism and poor perfusion of solid tumours leave an acidic tumour environment due to glycolysis under hypoxic conditions, which is perhaps the most pervasive tumour microenvironment regardless of the tumour types.[223] The relatively low pH was hypothesized to play an important role in promoting the local invasive growth and metastasis of cancers.[224, 225] Many pH-responsive materials have been designed as diagnostic[226-228] and therapeutic[229-232] tools targeting specifically to tumour. Using the concept of pH-driven drug delivery systems, PDT can be modulated as pH-responsive platforms through controlling the effectiveness of PSs at different pH values. These strategies can be divided into two categories: (i) chemically alternating the structure of PSs through pH-responsive (e.g., cleavable, protonation) modifications, which turn into activated

phototoxicity in acidic environment[233-237] and (ii) physically quenching the photodynamic effect of PSs by the FRET process, which can be destroyed by acidic stimulation.[238, 239]

O'Shea and colleagues described a supramolecular photonic therapeutic agent (SPTA) enabling reversible off/on switching of $^1O_2$ generation in response to external pH changes.[233] The intramolecular photoinduced electron transfer (PeT) initially decayed the excited state of PSs, resulting in virtually no $^1O_2$ generation upon light irradiation. Under acidic environment, the protonation of amine receptors of BF_2-chelated azadipyrromethenes would deactivate the ET and restore the $^1O_2$ generation ability upon light irradiation. Several other *in vivo* studies on pH-activatable PDT further demonstrated the potential of this strategy with possibly fewer side effects.[236, 237] Ju and Yu et al. reported an aza-boron-dipyrromethene (aza-BODIPY) structure substituted with diethylaminophenyl and bromophenyl (NEt_2Br_2BDP) as an acidic pH-activatable PS (**Fig. 16A**).[236] The nanoprobe is silent under physiological condition (pH 7.4), but is activated in the acidic environment (pH 4.5-5.0) to produce $^1O_2$ for efficient tumour therapy under 808 nm irradiation (**Fig. 16B, C**).[236]

Besides chemical variations, PSs can also be quenched by physical energy transferring strategy. In such a system, pH-responsive materials are introduced to control the degree of quenching efficiency and thereby the ROS generation of PSs. For example, Liu's group reported a micelle structure composed of PS-conjugated pH-responsive copolymers where fluorescence emission of PSs (eosin Y, EoS) was quenched by self-quenching and PeT process.[238] Under acidic environment associated with tumour endolysosomes, the protonation of poly (2-diisopropylamino) ethyl methacrylate tertiary amine moieties led to the micelle-to-unimer transition and the release of PSs. The restoring of fluorescence emission enables $^1O_2$ generation upon light irradiation, which confers synergistic phototoxicity along with photothermal effect. The similar concept of responsive PDT can be modulated by cooperating with inorganic nanostructures.[240]

4.3.3 Oxidative catalysis—Cancer cells are known to undergo an elevated oxidative stress during the fast proliferation and outgrowth.[1, 26] The increased metabolic activity and ROS generation have been recognized as site-specific stimuli combining the use of ROS-responsive materials.[241, 242] Because most of the currently available PSs undergo Type II photosensitization, the deactivation of intersystem crossing could attenuate the yield of triplet state, thus constraining the formation of $^1O_2$.

Cosa et al. designed a two-segment photosensitizer-trap molecule (Br_2B-PMHC) as a dormant $^1O_2$ PS which is deactivated due to the PeT from the trap segment to the PS segment, competing with the intersystem crossing.[243] Combined singlet and triplet quenching of the excited PS along with the physical quenching of $^1O_2$ by the chromanol ring of α-tocopherol of the trap segment provide three layers of suppression of $^1O_2$ production (**Fig. 17A**). However, oxidation of the trap segment by ROS would effectively restore the ability of the dormant PS to sensitize $^1O_2$ and abort its ability to scavenge $^1O_2$ species. This system with juxtaposed antioxidant and pro-oxidant antagonistic chemical activities for a dormant PS enables ROS-mediated activation of $^1O_2$ sensitization providing a new chemical solution for the spatiotemporal control of $^1O_2$ production. The selective photoactivation and

production of $^1O_2$ in ROS-stressed *vs.* regular cells were successfully tested *via* the photodynamic inactivation of a ROS-stressed Gram-negative *E. coli* strain (**Fig. 17B, C**). Another study by the same group reported a Chlorin e6-hyaluronic acid (Ce6-HA) conjugate that can be activated by peroxynitrite in macrophage cells.[244] In particular, significantly higher phototoxic effect was observed in the activated macrophage cells over human dermal fibroblasts and non-activated macrophages.

By using the elevated endogenous ROS levels to amplify exogenous ROS generation in cancer cells may promise minimal toxicity to healthy cells.[26] The realization of metabolic imbalance in cancer cells will open up new avenues to develop approaches enabling selective activation of the ROS generation while minimizing the damage to healthy cells.

4.3.4 Aptamer targets—Disease-specific ligands have been extensively explored to enhance the selectivity of therapeutic effects and reduce undesirable side effects in disease treatment.[245-247] One approach toward this goal is to utilize an antigen-antibody system to guide the specific delivery of drugs. As an emerging class of chemical targeting ligands, single-stranded oligonucleotides, known as aptamers, offer significant advantages to generate cancer-specific drug delivery systems, such as flexible design, synthetic accessibility, easy modification, chemical stability, and rapid tissue penetration.[248] Particularly, due to the conformational flexibility, aptamers can be programmed into FRET systems in which aptamers may change their conformation in the presence of specific targets to modulate the FRET efficiency.[249-251] In this regard, aptamer-based FRET systems may achieve activatable photosensitization with high specificity.[252, 253]

Tan and co-workers successfully constructed a PDT system that can be selectively triggered by target proteins based on aptamers and single-walled carbon nanotubes (SWNTs).[254] The aptamer-SWNT design was based on the attachment of PS-conjugated aptamers on SWNTs through π-π stacking between nucleotide bases and SWNT side walls. The quenching of $^1O_2$ generation in aptamer-SWNT was restored by a magnitude of 20 in the presence of specific target proteins (thrombin), which was achieved by the reduced proximity between PSs and SWNTs and the destroyed FRET events. This concept has provided a paradigmatic design for cancer-specific PDT based on the aptamer targeting approach.[255-257] In a more recent study, Hahn's group reported an RNA aptamer-conjugated PS (AIR-3A-Ce6) for specific binding to interleukin 6 receptor (IL-6R), which is a multifunctional cytokine involved in various diseases such as Crohn's disease, rheumatoid arthritis, psoriasis, systemic sclerosis, and some cancers.[258] The AIR-3A-Ce6 conjugate was rapidly and specifically internalized by IL-6R-positive BaF3/gp130/IL6R/TNF cells. As a result, the viability of IL-6R-positive cells was significantly inhibited under light irradiation due to ROS generation, while negligible cytotoxicity was found in IL-6R-negetive cells and cells treated with unconjugated Ce6 molecules.[258]

Overall, engineered aptamer conjugates hold great promise to specifically deliver PSs into target cancer cells and more importantly, specifically activate the photosensitization in cancer cells. One of the major concerns for aptamers, especially those developed against intracellular targets, is the intracellular stability. Unlike antibodies, the tertiary structure of aptamers is highly dependent on solution conditions. Hence, aptamers could lose their

binding affinity by the change of three-dimensional structure due to the complicated intracellular environment (e.g., pH, ionic strength). However, this problem can be partially addressed by increasing the diversity of nucleic acid pools through chemical modifications.[259, 260]

5. Genetically encoded photosensitizers

PSs used to date are predominantly derived from chemical synthesis. The challenges to deliver and remove exogenous PSs are still prevalent in PDT studies. Sophisticated design and synthesis of chemical PSs capable of targeting tumour cells, and more specifically, subcellular organelles have attracted considerable research interest. These strategies are expected to significantly enhance the PDT outcomes to tumour cells while minimizing PS dose and harmful side effects. For example, aptamer-based G-quadruplex (GQ) structure integrated with PSs have provided an efficient way to deliver PSs to target cells with high affinity and selectivity.[252] The formation of aptamer GQ structure by self-assembly can be stabilized by ligands through π–π stacking and electrostatic interactions, such as the use of PS molecules naphthalene diimides,[261, 262] perylene diimides,[263] and porphyrins.[264] Mitochondrion, as energy factory of cells, plays a pivotal role in arbitrating cell apoptosis which can be initiated by the elevated ROS level especially that is originated from the mitochondrion itself.[262] In addition, lysosomal targeted PSs to directly activate cell apoptosis and nuclear targeted PSs to introduce *in situ* double strand breaks and alkali-labile lesions in the DNA molecules have been widely studied. Organelle-targeted PSs that specifically accumulate in hypersensitive subcellular locations, such as nucleus,[265, 266] lysosome,[267] and mitochondrion,[268, 269] have provided an elevated level of controllable photosensitization. These approaches on whether and to what extent subcellular localization of PSs may influence the overall efficiency of photodynamic therapy have been concisely studied and summarized.[270, 271]

Although significant improvements have been made to provide controllable photosensitization specifically on tumour area and in specific organelles, these strategies still show some off-target effect from nonspecific localization.[76] More severely, mitochondria targeted PSs have been found with high dark toxicity probably due to the highly cationic nature of the molecules in order to cross mitochondrial membrane of negative potential.[270, 271] Nuclear targeted PSs are also not favorable due to the high risk of causing genetic variation.[269] Therefore, selectively targeting and activating PSs with high specificity and low potential of side effect remain an important goal in PDT-associated cancer therapy.

5.1 KillerRed

Genetically encoded fluorescent proteins (FPs) have been widely developed as a general tool for microscopy.[272, 273] Specifically, FPs that generate $^1O_2$ are of special interest for correlative light and electron microscopy.[274] Recently, genetically encoded ROS-generating proteins (RGPs) have been recognized as phototoxic cancer therapeutic agents, propagating the family of PSs.[275] For example, fluorescent proteins such as green fluorescence protein (GFP) can be used as site-specific labels for cell, organelle, and protein, which may also

photosensitize $^1O_2$ but at a very low efficiency.[276] The photochemically inert nature of GFP is probably due to the shielded chromophore in their structure.[277]

Photochemically active versions of GFP have been developed using transgenic technologies, which were employed for exerting phototoxic effect and cancer cell ablation.[274, 278-280] On the other hand, reducing irradiance and/or fluence can achieve sub-lethal levels of ROS for mediating subtle cellular signaling.[277] The first developed RGP was the KillerRed, a homolog of GFP, anm2CP, by Lukyanov and coworkers.[275] The structure of KillerRed has a unique water-filled channel reaching the chromophore, which may be responsible for its prominent phototoxic nature over original GFP. KillerRed is known to produce $O_2^{\bullet -}$ via a type I photosensitization upon irradiation with red light. In a recent study, KillerRed was fused to an antibody to target tumour cells.[281] The resulting photo-induced ROS generation led to tumour-specific cell death, suggesting that genetically encoded RGPs may be useful for enhanced PDT while circumventing the limited specificity of synthetic PSs.[281] However, the dimerization tendency of KillerRed largely prevents its fusion with proteins of interest, thus hindering its wide applications. Recently, SuperNova, a monomeric RGP, was generated through random mutagenesis of KillerRed.[282] In contrast to KillerRed, SuperNova in fusion with target proteins showed proper localization and little perturbation to mitotic cell division, which could to some extent overcome the major drawbacks of KillerRed.[282] The ROS generation responsible for the phototoxic effects of SuperNova remains to be elucidated, because both $O_2^{\bullet -}$ and $^1O_2$ were detected during the photosensitizing reactions.

5.2 MiniSOG

Recent efforts to develop genetically encodable tags enabling to generate $^1O_2$ have been focused on flavin mononucleotide (FMN)-binding FPs,[280] because FMN is an efficient PS with relatively high quantum yield in photosensitizing $^1O_2$ (Φ = 0.51). MiniSOG (abbreviation of mini singlet oxygen generator) is a green fluorescent flavoprotein derived from phototropin 2 containing 106 amino acids.[272] The excitation spectrum is maximized at 488 nm with Φ of approximately 0.47, basically equal to that of free FMN.[272] The miniSOG monomers are capable of generating $^1O_2$ but not $O_2^{\bullet -}$, indicating that this procedure occurs through a type II photosensitization. The flavin mononucleuotide cofactor required by miniSOG is endogenously present in cells, making it a suitable candidate for correlative electron microscopy. The size of miniSOG is less than one quarter the size of the obligate dimer of KillerRed, and less than half the size of GFP.[272, 274] Because of this distinguishing feature, miniSOG facilitates protein tagging and is less likely to influence protein targeting than larger tags.[280]

Upon blue light illumination, miniSOG generates a sufficient quantity of $^1O_2$ which was capable of catalyzing local polymerization of diaminobenzidine into precipitates for imaging by electron microscopy.[272] Tsien and Jin et al. demonstrated that mitochondrial targeted miniSOG is a potent light-induced cell ablation reagent in *C. elegans*.[274] Another study employed genetically encoded immune-PS 4D5scFv-miniSOG to selectively recognize the extracellular domain of human epidermal growth factor receptor 2 (HER2/neu), a receptor overexpressed in many human carcinomas.[283] The recombinant protein 4D5scFv-miniSOG exerted a highly specific photo-induced cytotoxic effect on HER2/neu-positive SK-BR-3

human breast adenocarcinoma cells (IC_{50} = 160 nM).[283] However, blue light has limited propagation through the tissue and may hinder the wide applications of miniSOG in clinical practice. In this regard, future studies might require light delivery systems to permit interstitial activation of miniSOG for in-depth PDT, as described in Section 2.

5.3 NIR light-excitable protein

To gain more clinical relevance, PSs are required to be excited with NIR light for deep tissue penetration. However, most of the current genetically encoded RGPs are below this spectral range, causing concern about the undesirable photosensitization by endogenous chromophores. Recently, Bruchez's group produced an NIR light-excitable fluorescent complex by a targeted and activated photosensitizer (TAP) and a genetically encoded fluorogen-activating protein (FAP).[284] TAP is an iodine-substituted malachite green (MG) analog with low free fluorescence and ROS generation, while FAP is a genetically encoded fluorogen with dL5** (a 25-kDa binder) moiety specifically binding to MG derivatives. The heavy-atom substitution is to increase intersystem crossing and redshift the major absorption band of the MG chromophore (**Fig. 18A**). The association and formation of FAP-TAPs produce $^1O_2$ with high quantum yield (Φ = 0.13) when activated at 666 nm, whereas the control MG-ester-dL5** or free TAPs dye showed no detectable $^1O_2$ generation under the same conditions.[284] This targeted and activated approach enables $^1O_2$-mediated protein inactivation, targeted cell killing and rapid targeted lineage ablation in living larva and adult zebrafish (**Fig. 18B, C**). Remarkably, the NIR excitation and emission of this FAP-TAPs provide a new spectral range for RGPs that could be useful for manipulating cellular ablation deep within living organisms.

Although genetically encoded photosensitizers for PDT study can allow photosensitization with high precision, current studies are mostly limited at a proof-of-concept level *in vitro*. This approach is based on the genetic transfection and expression of specific fluorophores in cells, which could face a major gap between *in vitro* study and *in vivo* applications. An *in vivo* study showed that intratumoral injection of gene complexes can efficiently eliminate tumours upon laser irradiation.[278] In this respect, genetically encoded photosensitizers have great potential to achieve tumour-specific PDT provided by the efficient gene delivery, transfection, and expression in tumour cells.

6. Non-photodynamic approaches

The excessive production of ROS in cancer cells that overwhelms their eliminating capability can cause toxicity to cells.[11] The cascade damages would happen irreversibly once the intracellular ROS reaches a level higher than cells can tolerate, causing apoptosis or necrosis depending on the dose. Therefore, one may conclude that introduction of ROS to cells with a considerable level may exert toxicity to cells. Drug developments based on this rationale have been applied to a broad scale of anticancer drugs.[285]

PDT provides an effective way to kill cancer cells through a ROS-mediated mechanism. Besides PSs, a lot of other chemicals have been found to generate a high level of ROS in a non-photodynamic manner in cells. In contrast to photosensitization, non-photodynamic ROS generation without the need of light, oxygen, and PSs have been demonstrated as an

alternative strategy for cancer therapy. The approaches that induce non-photodynamic ROS generation can be categorized into the following categories: (i) molecular drugs; (ii) nanomaterials; and (iii) biochemical reactions. Regardless of the spatiotemporal control of ROS generation, this strategy modulating the unique redox regulatory mechanisms of cancer cells could have major implications in cancer treatments.

6.1 Molecular drugs

One common drug that can generate ROS is procarbazine, which produces H_2O_2 through oxidation in aqueous solution and has been used for the treatment of Hodgkin's lymphoma and primary brain cancers.[286] It is noted that procarbazine can cause DNA methylation, which would generate the replication-blocking and mispairing lesions.[287] The formation of H_2O_2 is essential to exert the cytotoxic effects following chain reactions to produce highly toxic radicals.[288] This process can happen without light activation, leading to an elevated ROS level and degradation to nuclear DNA fragments.[286] Since the first approval by FDA in 1969, the case of procarbazine has promoted extensive exploitation of ROS-mediated therapeutic options, such as arsenic trioxide and parthenolide.[285, 286, 289]

Doxorubicin, a widely used redox-cycling anthracycline drug, is known to generate ROS by several different mechanisms.[285] First, doxorubicin may interact with trace metals, such as iron (III), to produce iron (II)-doxorubicin free radical, which could reduce molecular oxygen to $^1O_2$.[290, 291] Second, doxorubicin can be reduced by one electron mechanism via mitochondrial reductases to anthracycline semiquinone free radicals, which in turn reduce molecular oxygen to $O_2^{\bullet-}$ and H_2O_2 under aerobic conditions.[292] Cisplatin-based drugs are also able to generate ROS through nicotinamide adenine dinucleotide phosphate hydrogen (NADPH) oxidase mechanism.[293] However, there is no evidence that elevated ROS levels upon treatment by these molecular drugs are dose-dependent, nor the significant contribution to anticancer effects. The anticancer activities for these molecular drugs are still dominated by the formation of intra-strand DNA cross-links.

ROS generation during chemotherapy could be involved in a variety of cellular signaling pathways.[285] The common ground is that ROS can alter enzyme functions and protein structures causing cell death by the apoptotic or necrotic pathway, and the related mechanisms and outcomes may vary among different cell types, doses, and drug variations.[294] Molecular drugs that are able to generate ROS in cells could be a way to guide the mechanistic study on the ROS mediated cellular activity and potential anticancer activity of these molecular drugs. Further studies about the mechanistic illustration of molecular drug-inducible ROS generation are needed to have a major impact on anticancer drug development.[286]

6.2 Nanomaterials

The emergence of nanotechnology and nanomedicine offers vast opportunities in biomedical engineering and disease treatments. In this regard, modulating the structural and physicochemical properties of nanomaterials can lead to significant changes in biological activities including ROS generation.[295] Oxidative stress induced by nanomaterials could be due to intrinsic aspects of nanomaterials, such as surface, size, composition, and shape;

cellular responses to nanomterials such as mitochondrial respiration, nano-bio interfacial interaction, and immune cell activation are responsible for ROS-mediated damage.[296, 297]

Due to the large array of π-π conjugated structure, single-walled carbon nanotubes (SWCNTs) can enhance electrochemical reactivity of certain biomolecules and promote electron-transfer reactions in proteins.[298-300] In other words, SWCNTs can act as redox mediators by shuttling electrons from biological electron donors (i.e., reducing agents) to electron acceptors (i.e., oxidizing agents).[301, 302] Therefore, SWCNTs can be considered as solid matrices in different Fermi levels depending on the number of electrons transferred to each SWCNT. Previous studies have shown that carbon-based nanomaterials are efficient PSs to produce ROS under light-activated photodynamic procedure for cancer therapy.[303-307] A study by Wang and Zhang et al reported that graphene quantum dots (GQDs) exhibited a high $^1O_2$ generation yield, greater than 1.3, through a multistate sensitization (MSS) mechanism.[308] Recently, Jafvert's group reported that carboxylated SWCNT (C-SWCNT) were able to generate ROS in the dark.[302] The study indicated that C-SWCNTs initially store the electrons transferred from both NADH (β-nicotinamide adenine dinucleotide, reduced form) and DTTre (DL-dithiothreitol, reduced form)and subsequently shuttle these electrons to molecular oxygen-generating $O_2\bullet^-$ species. The electron transferring efficiency of CNTs is highly dependent on the surface coating and dispersive ability in the water.[301] These results indicate that C-SWCNTs can be a light-independent source of ROS in water by oxidation of electron donors. Thus, the electron shuttling through CNTs to molecular oxygen may be a potential mechanism for DNA damage by various carbon-based nanomaterials.[309]

Cancer cells incubated with silver (Ag) nanomaterials were found to undergo significant oxidative stress with a more than 10-fold increase of ROS level in cells exposed to 50 μg/mL Ag-15nm NPs, indicating that the cytotoxicity could be related to the ROS-mediated mechanism.[310] Interestingly, cell viability increases with increasing the size of Ag NPs. Only marginal toxicity was observed when cells were incubated with Ag-55 nm NPs, which could be attributed to the decreased reactive nature of NPs with a relatively large size.[310] Yang's group explored the surface chemistry of copper (Cu) NPs with a diameter of 15 nm during and after ROS generation in a non-cellular assay.[311] Transmission electron microscopy (TEM), powder X-ray diffraction (PXRD) and UV-vis spectroscopy were used to identify that ROS generation is closely related to the surface oxidation of Cu NPs. Longer chain ligands could better protect Cu NPs from oxidation and lead to lower ROS generation than Cu NPs with shorter chain ligands on the surface. These studies implied that ROS-mediated potential toxicity by nanomaterials is an integrative effect intimately related to their physiochemical features, which could be an important guideline to develop nanomaterials for medical applications.[295, 312]

6.3 Biochemical reactions

Mitochondria are the most important organelles responsible for the production of $O_2\bullet^-$ by one-electron reduction of O_2 molecule. $O_2\bullet^-$ is the main precursor of most highly oxidizing or reducing species to initiate oxidative cascades in the cell.[4, 16] In fact, ROS are constantly produced as by-products in a series of biochemical reactions during cell metabolism. For

example, dismutation of $O_2\bullet^-$ by superoxide dismutases (e.g., MnSOD, Cu/ZnSOD) produces H_2O_2, which in turn may be fully reduced to water or partially reduced to HO•, one of the strongest oxidants in nature. In addition, $O_2\bullet^-$ may react with other radicals including nitric oxide (NO•), which produces another powerful oxidant, peroxynitrite, propagating the family of reactive nitrogen species (RNS). Although cells have several mechanisms to eliminate the overproduced reactive species maintaining their oxidative balance, overwhelming the imbalance between ROS generation and elimination is an efficient strategy to kill cancer cells.[26] In fact, apoptotic procedures for cells at the late life stage could be partially ascribed to the amplified ROS generation which surpasses the capability of eliminating them. Therefore, it is reasonable to assume that engineered biochemical reactions enabling the on-demand production of ROS in cancer cells may have great potential to trigger cell death. Recently, a number of approaches based on this assumption have been described, such as Fenton reaction.[205,313]

6.3.1 Fenton reaction—HO• is the most reactive radical that is produced mainly through the Fenton reaction from H_2O_2 and metal species (e.g., iron, copper), while Haber-Weiss reaction also serves as HO• source from $O_2\bullet^-$ and H_2O_2 but in a much slower manner. HO• can successively react with biomolecules at a diffusion-controlled rate to form a series of additional free radicals, for examples, thiyl (RS•), carbon-centred ($(R)_3C\bullet$), and peroxyl radicals ($(R)_3COO\bullet$), which may cause considerable damage to cells.[314] As many cancer cells overproduce H_2O_2, this accumulative nature has been exploited to implement specific therapeutic strategies, such as to spontaneously trigger responsive-drug release for chemotherapy or to stimulate endogenous O_2 production for enhanced photodynamic therapy.[315-317]

To explore the potential for cancer therapy based on Fenton reaction-produced ROS, Shi and colleagues reported a hubble-bubble approach to synthesize amorphous iron nanoparticles (AFe-NPs). These NPs were rapidly ionized in acidic tumours for the on-demand release of Fe^{2+} ions and enabled subsequent localized Fenton reaction for specific cancer therapy (**Fig. 19A**).[313] The AFe-NPs showed remarkable advantages over the corresponding crystalline iron nanocrystals (FeNCs) in cancer therapy benefiting from their amorphous nature. This chemodynamic therapy (CDT) paradigm that combines the specific property of cargo and tumour microenvironment promises efficient on-demand generation of HO• from H_2O_2 (**Fig. 19B, C**). Another study that employed H_2O_2-filled polymersome to show ROS-mediated cancer therapy based on Fenton reaction has been reviewed in section 4.2, which displayed echogenic reflectivity by US induced disruption of PLGA polymersome.[205] In this regard, CDT can be an alternative tool for ROS generation internalized by endogenous chemical energy without the need for external input of laser irradiation or local oxygen, thus circumventing the limitations posed by the penetration depth of light through tissues and the hypoxic tumour environment.[205, 313]

Besides iron, other transition metals or nanostructures, such as manganese, copper, cobalt, cerium, and nonmetallic carbon can catalyze the Fenton or Fenton-like reaction.[318-320] External energy inputs including photo-, sono-, or electro-assisted Fenton reactions have been widely studied as well.[321] These portraits may provide versatile cut-in points of employing Fenton reaction to generate ROS for specific cancer therapy.[322] Although still in

its infancy, the development of cancer-specific Fenton reaction taking advantages of the discrepancy between cancer microenvironment and normal tissues may open up new avenues to treat cancer cells through engineered biochemical reactions.

6.3.2 Others—In biological systems, ROS can be produced in a series of light-dependent and -independent manners. This category of biochemical routes in terms of generation and biological significance of ROS have been reviewed elsewhere.[214, 323, 324] Taking $^1O_2$ for example, which is the major cytotoxic species in eukaryotic cells, light-independent production of $^1O_2$ during the cell life cycle would happen between i) H_2O_2 and hypochlorite (ClO^-) during phagocytosis, ii) electron transfer reaction from excited carbonyl species, iii) superoxide anion reactions with organic or inorganic substances, iv) ozone reaction involving hydrotrioxide intermediates, v) peroxynitrite reactions with hydroperoxides or hydrogen peroxides, vi) decomposition of lipid hydroperoxides by reduction through Russell mechanism, and vii) enzymes (e.g., catalase, peroxidases) involved in metabolism, and so on.[323-325] The major routes and substances for $^1O_2$ generation in biological systems are displayed in **Fig. 20**.

Modulation of these biochemical reactions has been widely studied in cell biology to understand their cellular functions and impacts, which are especially important to guide the cancer therapy based on ROS-mediated mechanism. These biochemical reactions can be operated as pro-drug activatable systems for non-photodynamic ROS generation by specific stimulations (e.g., pH or redox) in cancer cells. However, so far very few biochemical reactions have been engineered as ROS sources for cancer treatment. The major challenges for this nascent concept are multifold: (i) to generate ROS specifically in cancer cells, and to a much lesser extent in normal cells; (ii) to produce sufficient ROS for inducing damage to cancer cells; and (iii) to stabilize pro-drug intermediates in an ambient environment. Remarkably, the emergence of nanotechnology and nanomedicine may provide a series of toolboxes to materialize this particular approach.[326-329] Therefore, we look forward to witnessing the breakthrough of engineered non-photodynamic ROS generation for cancer therapy through interdisciplinary collaborations between chemistry, material science, nanotechnology, nanomedicine, and oncology.

7. Conclusion and perspective

The past decades have witnessed tremendous developments of PDT due to its feasibility in cancer treatment. The underlying mechanism of PDT for growth inhibition and shrinkage of tumours is the generation of ROS. Although PDT drugs have been approved for clinical use, it has not gained acceptance as a first-line treatment option. Recent advances in nanotechnology and nanomedicine have opened up an extremely promising avenue in the field of PDT providing versatile technological opportunities to encounter the existing challenges of PDT systems. In this review, we have attempted to provide an overview of a variety of approaches to generate ROS for cancer therapy. The judicious designs were categorized taking into consideration the following aspects: (i) introducing engineered light source for in-depth penetration; (ii) constructing oxygen self-supplied formulations; (iii) making photosensitization responsive to diverse stimulations other than light; (iv)

programing genetically encodable PSs; and (v) utilizing non-photodynamic biochemical reactions to avoid the dependence on PSs, oxygen and light.

By surveying the existing literature, we firmly believe that rationally engineered ROS generation strategies will expand our cancer treatment options. Due to the lack of clinical evidence, however, most of the developed ROS generation systems are still in the early development stage. Future work should focus on the following important questions: (i) how to delimitate the functional ROS levels during photodynamic or non-photodynamic cancer therapy, (ii) how to precisely control ROS generation specifically in the tumour but not in normal cells, and (iii) how to clinically translate the new ROS generation approaches to target deep-seated tumors. We hope that this review is timely in providing an overview of current status on this theme and will shed new light on future directions to move forward in the continued battle to conquering cancer.

Supplementary Material

Refer to Web version on PubMed Central for supplementary material.

Acknowledgements

References

1. Dickinson BC, Chang CJ. Nat. Chem. Biol. 2011; 7:504–511. [PubMed: 21769097]
2. Apel K, Hirt H. Annu. Rev. Plant Biol. 2004; 55:373–399. [PubMed: 15377225]
3. Tripathy BC, Oelmüller R. Plant Signal. Behav. 2012; 7:1621–1633. [PubMed: 23072988]
4. Turrens JF. J. Physiol. 2003; 552:335–344. [PubMed: 14561818]
5. Murphy, Michael P. Biochem. J. 2009; 417:1–13. [PubMed: 19061483]
6. Ray PD, Huang B-W, Tsuji Y. Cell Signal. 2012; 24:981–990. [PubMed: 22286106]
7. Schumacker, Paul T. Cancer Cell. 2015; 27:156–157. [PubMed: 25670075]
8. Finkel T. J. Cell Biol. 2011; 194:7–15. [PubMed: 21746850]
9. Flannagan RS, Cosio G, Grinstein S. Nat. Rev. Micro. 2009; 7:355–366.
10. Cairns RA, Harris IS, Mak TW. Nat. Rev. Cancer. 2011; 11:85–95. [PubMed: 21258394]
11. Ramsey MR, Sharpless NE. Nat. Cell Biol. 2006; 8:1213–1215. [PubMed: 17077852]
12. Takahashi A, Ohtani N, Yamakoshi K, Iida S.-i. Tahara H, Nakayama K, Nakayama KI, Ide T, Saya H, Hara E. Nat. Cell Biol. 2006; 8:1291–1297. [PubMed: 17028578]
13. Szatrowski TP, Nathan CF. Cancer Res. 1991; 51:794–798. [PubMed: 1846317]
14. Kawanishi S, Hiraku Y, Pinlaor S, Ma N. Biol. Chem. 2006; 387:365–372. [PubMed: 16606333]
15. Toyokuni S, Okamoto K, Yodoi J, Hiai H. Febs. Lett. 1995; 358:1–3. [PubMed: 7821417]
16. Sabharwal SS, Schumacker PT. Nat. Rev. Cancer. 2014; 14:709–721. [PubMed: 25342630]
17. Liou G-Y, Storz P. Free. Radical. Res. 2010; 44 10.3109/10715761003667554.
18. Shazib P, Marie-Veronique C. Curr. Pharma. Des. 2004; 10:1969–1977.
19. Tiligada E. Endocr-relat. Cancer. 2006; 13:S115–S124. [PubMed: 17259552]
20. Richard S, Charles HG. Curr. Pharm. Design. 2008; 14:1113–1123.

21. Trachootham D, Zhou Y, Zhang H, Demizu Y, Chen Z, Pelicano H, Chiao PJ, Achanta G, Arlinghaus RB, Liu J, Huang P. Cancer Cell. 2006; 10:241–252. [PubMed: 16959615]

22. Niu C, Yan H, Yu T, Sun H-P, Liu J-X, Li X-S, Wu W, Zhang F-Q, Chen Y, Zhou L, Li J-M, Zeng X-Y, Yang R-RO, Yuan M-M, Ren M-Y, Gu F-Y, Cao Q, Gu B-W, Su X-Y, Chen G-Q, Xiong S-M, Zhang T.-d. Waxman S, Wang Z-Y, Chen Z, Hu J, Shen Z-X, Chen S-J. Blood. 1999; 94:3315–3324. [PubMed: 10552940]

23. Soignet SL, Maslak P, Wang Z-G, Jhanwar S, Calleja E, Dardashti LJ, Corso D, DeBlasio A, Gabrilove J, Scheinberg DA, Pandolfi PP, Warrell RPJ. New Engl. J. Med. 1998; 339:1341–1348. [PubMed: 9801394]

24. Attia S, Kolesar J, Mahoney MR, Pitot HC, Laheru D, Heun J, Huang W, Eickhoff J, Erlichman C, Holen KD. Invest. New Drug. 2008; 26:369–379.

25. Ramanathan B, Jan K-Y, Chen C-H, Hour T-C, Yu H-J, Pu Y-S. Cancer Res. 2005; 65:8455–8460. [PubMed: 16166325]

26. Trachootham D, Alexandre J, Huang P. Nat. Rev. Drug Discov. 2009; 8:579–591. [PubMed: 19478820]

27. Beel JA, Lillehei KO. Med. Hypotheses. 2000; 55:29–35. [PubMed: 11021322]

28. Fiona HF, Claus J. Curr. Pharm. Design. 2006; 12:4479–4499.

29. Pelicano H, Carney D, Huang P. Drug Resist. Update. 2004; 7:97–110.

30. Kong Q, Lillehei KO. Med. Hypotheses. 2006; 51:405–409.

31. Agostinis P, Berg K, Cengel KA, Foster TH, Girotti AW, Gollnick SO, Hahn SM, Hamblin MR, Juzeniene A, Kessel D, Korbelik M, Moan J, Mroz P, Nowis D, Piette J, Wilson BC, Golab J. CA Cancer J. Clin. 2011; 61:250–281. [PubMed: 21617154]

32. Clare C, Stanley BB. CRC Handbook of Organic Photochemistry and Photobiology, Third Edition - Two Volume Set. 2012:1511–1528. CRC Press.

33. JulieTzu-Wen W, Josephine HW, Alexander JM, Stephen GB, Kristian B. CRC Handbook of Organic Photochemistry and Photobiology, Third Edition - Two Volume Set. 2012:1529–1540. CRC Press.

34. Dougherty TJ, Grindey GB, Fiel R, Weishaupt KR, Boyle DG. J. Natl. Cancer I. 1975; 55:115–121.

35. Dougherty TJ, Gomer CJ, Henderson BW, Jori G, Kessel D, Korbelik M, Moan J, Peng Q. J. Natl. Cancer I. 1998; 90:889–905.

36. Dolmans DEJGJ, Fukumura D, Jain RK. Nat. Rev. Cancer. 2003; 3:380–387. [PubMed: 12724736]

37. Allison RR, Mota HC, Sibata CH. Photodiagnosis Photodyn. Ther. 2004; 1:263–277. [PubMed: 25048431]

38. Cheng L, Wang C, Feng L, Yang K, Liu Z. Chem. Rev. 2014; 114:10869–10939. [PubMed: 25260098]

39. Lucky SS, Soo KC, Zhang Y. Chem. Rev. 2015; 115:1990–2042. [PubMed: 25602130]

40. Wilson B. Can. J. Gastroenterol Hepatol. 2002; 16:393–396.

41. Brian CW, Michael SP. Phys. Med. Biol. 2008; 53:R61. [PubMed: 18401068]

42. Bonnett R. Chem. Soc. Rev. 1995; 24:19–33.

43. Kamkaew A, Lim SH, Lee HB, Kiew LV, Chung LY, Burgess K. Chem. Soc. Rev. 2013; 42:77–88. [PubMed: 23014776]

44. Ethirajan M, Chen Y, Joshi P, Pandey RK. Chem. Soc. Rev. 2011; 40:340–362. [PubMed: 20694259]

45. Brown SB, Brown EA, Walker I. Lancet Oncol. 2004; 5:497–508. [PubMed: 15288239]

46. Huang Z. Technol. Cancer Res. Treat. 2005; 4:283–293. [PubMed: 15896084]

47. Sandell JL, Zhu TC. J. Biophotonics. 2011; 4:773–787. [PubMed: 22167862]

48. Steven LJ. Phys. Med. Biol. 2013; 58:R37. [PubMed: 23666068]

49. Hu J, Tang Y. a. Elmenoufy AH, Xu H, Cheng Z, Yang X. Small. 2015; 11:5860–5887. [PubMed: 26398119]

50. Smith AM, Mancini MC, Nie S. Nat. Nanotechnol. 2009; 4:710–711. [PubMed: 19898521]

51. Luo S, Zhang E, Su Y, Cheng T, Shi C. Biomaterials. 2011; 32:7127–7138. [PubMed: 21724249]

52. Hong G, Diao S, Chang J, Antaris AL, Chen C, Zhang B, Zhao S, Atochin DN, Huang PL, Andreasson KI, Kuo CJ, Dai H. Nat. Photon. 2014; 8:723–730.

53. Idris NM, Jayakumar MKG, Bansal A, Zhang Y. Chem. Soc. Rev. 2015; 44:1449–1478. [PubMed: 24969662]

54. Wang C, Cheng L, Liu Z. Theranostics. 2013; 3:317–330. [PubMed 23650479]

55. Wolfbeis OS. Chem. Soc. Rev. 2015; 44:4743–4768. [PubMed: 25620543]

56. Park YI, Lee KT, Suh YD, Hyeon T. Chem. Soc. Rev. 2015; 44:1302–1317. [PubMed: 25042637]

57. Chan EM, Levy ES, Cohen BE. Adv. Mater. 2015; 27:5753–5761. [PubMed: 25809982]

58. Zhou J, Liu Q, Feng W, Sun Y, Li F. Chem. Rev. 2015; 115:395–465. [PubMed: 25492128]

59. Chen G, Qiu H, Prasad PN, Chen X. Chem. Rev. 2014; 114:5161–5214. [PubMed: 24605868]

60. Fan W, Bu W, Shi J. Adv. Mater. 2016 10.1002/adma.201505678.

61. So M-K, Xu C, Loening AM, Gambhir SS, Rao J. Nat. Biotech. 2006; 24:339–343.

62. Kamkaew A, Chen F, Zhan Y, Majewski RL, Cai W. ACS Nano. 2016; 10:3918–3935. [PubMed: 27043181]

63. Ding Y, Wu F, Zhang Y, Liu X, de Jong EMLD, Gregorkiewicz T, Hong X, Liu Y, Aalders MCG, Buma WJ, Zhang H. J. Phy. Chem. Lett. 2015; 6:2518–2523.

64. Zhou B, Shi B, Jin D, Liu X. Nat. Nanotechnol. 2015; 10:924–936. [PubMed: 26530022]

65. Dong H, Du S-R, Zheng X-Y, Lyu G-M, Sun L-D, Li L-D, Zhang P-Z, Zhang C, Yan C-H. Chem. Rev. 2015; 115:10725–10815. [PubMed: 26151155]

66. Liu Y, Su Q, Zou X, Chen M, Feng W, Shi Y, Li F. Chem. Commun. 2016; 52:7466–7469.

67. Peng J, Guo X, Jiang X, Zhao D, Ma Y. Chem. Sci. 2016; 7:1233–1237.

68. Massaro G, Hernando J, Ruiz-Molina D, Roscini C, Latterini L. Chem. Mater. 2016; 28:738–745.

69. Liu K, Liu X, Zeng Q, Zhang Y, Tu L, Liu T, Kong X, Wang Y, Cao F, Lambrechts SAG, Aalders MCG, Zhang H. ACS Nano. 2012; 6:4054–4062. [PubMed: 22463487]

70. Zhou A, Wei Y, Wu B, Chen Q, Xing D. Mol. Pharma. 2012; 9:1580–1589.

71. Zhao Z, Han Y, Lin C, Hu D, Wang F, Chen X, Chen Z, Zheng N. Chem. Asian J. 2012; 7:830–837. [PubMed: 22279027]

72. Qiao X-F, Zhou J-C, Xiao J-W, Wang Y-F, Sun L-D, Yan C-H. Nanoscale. 2012; 4:4611–4623. [PubMed: 22706800]

73. Punjabi A, Wu X, Tokatli-Apollon A, El-Rifai M, Lee H, Zhang Y, Wang C, Liu Z, Chan EM, Duan C, Han G. ACS Nano. 2014; 8:10621–10630. [PubMed: 25291544]

74. Peng Q, Berg K, Moan J, Kongshaug M, Nesland JM. Photochem. Photobiol. 1997; 65:235–251. [PubMed: 9066303]

75. Peng Q, Warloe T, Berg K, Moan J, Kongshaug M, Giercksky K-E, Nesland JM. Cancer. 1997; 79:2282–2308. [PubMed: 9191516]

76. Lovell JF, Liu TWB, Chen J, Zheng G. Chem. Rev. 2010; 110:2839–2857. [PubMed: 20104890]

77. Park YI, Kim HM, Kim JH, Moon KC, Yoo B, Lee KT, Lee N, Choi Y, Park W, Ling D, Na K, Moon WK, Choi SH, Park HS, Yoon S-Y, Suh YD, Lee SH, Hyeon T. Adv. Mater. 2012; 24:5755–5761. [PubMed: 22915170]

78. Lin J, Wang S, Huang P, Wang Z, Chen S, Niu G, Li W, He J, Cui D, Lu G, Chen X, Nie Z. ACS Nano. 2013; 7:5320–5329. [PubMed: 23721576]

79. Wang C, Tao H, Cheng L, Liu Z. Biomaterials. 2011; 32:6145–6154. [PubMed: 21616529]

80. Wang M, Chen Z, Zheng W, Zhu H, Lu S, Ma E, Tu D, Zhou S, Huang M, Chen X. Nanoscale. 2014; 6:8274–8282. [PubMed: 24933297]

81. Chen F, Zhang S, Bu W, Chen Y, Xiao Q, Liu J, Xing H, Zhou L, Peng W, Shi J. Chem. Eur. J. 2012; 18:7082–7090. [PubMed: 22544381]

82. Guo H, Qian H, Idris NM, Zhang Y. Nanomed. Nanotech. Biol. Med. 2010; 6:486–495.

83. Idris NM, Gnanasammandhan MK, Zhang J, Ho PC, Mahendran R, Zhang Y. Nat. Med. 2012; 18:1580–1585. [PubMed: 22983397]

84. Qian HS, Guo HC, Ho PC-L, Mahendran R, Zhang Y. Small. 2009; 5:2285–2290. [PubMed: 19598161]

85. Zhang P, Steelant W, Kumar M, Scholfield M. J. Am. Chem. Soc. 2007; 129:4526–4527. [PubMed: 17385866]

86. Linsebigler AL, Lu G, Yates JT. Chem. Rev. 1995; 95:735–758.

87. Schwarz PF, Turro NJ, Bossmann SH, Braun AM, Wahab A-MAA, Dürr H. J. Phys. Chem. B. 1997; 101:7127–7134.

88. Boehm HP. Disc. Faraday Soc. 1971; 52:264–275.

89. Idris NM, Lucky SS, Li Z, Huang K, Zhang Y. J. Mater. Chem. B. 2014; 2:7017–7026.

90. Lucky SS, Muhammad Idris N, Li Z, Huang K, Soo KC, Zhang Y. ACS Nano. 2015; 9:191–205. [PubMed: 25564723]

91. Oheim M, Michael DJ, Geisbauer M, Madsen D, Chow RH. Adv. Drug Delivery Rev. 2006; 58:788–808.

92. Goyan RL, Cramb DT. Photochem. Photobiol. 2000; 72:821–827. [PubMed: 11140272]

93. Gallavardin T, Maurin M, Marotte S, Simon T, Gabudean A-M, Bretonniere Y, Lindgren M, Lerouge F, Baldeck PL, Stephan O, Leverrier Y, Marvel J, Parola S, Maury O, Andraud C. Photochem. Photobiol. Sci. 2011; 10:1216–1225. [PubMed: 21499638]

94. Qian J, Wang D, Cai F, Zhan Q, Wang Y, He S. Biomaterials. 2012; 33:4851–4860. [PubMed: 22484045]

95. Starkey JR, Rebane AK, Drobizhev MA, Meng F, Gong A, Elliott A, McInnerney K, Spangler CW. Clin. Cancer Res. 2008; 14:6564–6573. [PubMed: 18927297]

96. Collins HA, Khurana M, Moriyama EH, Mariampillai A, Dahlstedt E, Balaz M, Kuimova MK, Drobizhev M, YangVictor XD, Phillips D, Rebane A, Wilson BC, Anderson HL. Nat. Photon. 2008; 2:420–424.

97. Gallavardin T, Armagnat C, Maury O, Baldeck PL, Lindgren M, Monnereau C, Andraud C. Chem. Commun. 2012; 48:1689–1691.

98. Lanoe P-H, Gallavardin T, Dupin A, Maury O, Baldeck PL, Lindgren M, Monnereau C, Andraud C. Org. Biomol. Chem. 2012; 10:6275–6278. [PubMed: 22744649]

99. Dichtel WR, Serin JM, Edder C, Fréchet JMJ, Matuszewski M, Tan L-S, Ohulchanskyy TY, Prasad PN. J. Am. Chem. Soc. 2004; 126:5380–5381. [PubMed: 15113208]

100. Dini D, Calvete MJF, Hanack M, Amendola V, Meneghetti M. J. Am. Chem. Soc. 2008; 130:12290–12298. [PubMed: 18722439]

101. Ogawa K, Ohashi A, Kobuke Y, Kamada K, Ohta K. J. Am. Chem. Soc. 2003; 125:13356–13357. [PubMed: 14583021]

102. Fan Y, Liu H, Han R, Huang L, Shi H, Sha Y, Jiang Y. Sci. Rep. 2015; 5:9908. [PubMed: 25909393]

103. Chen C-L, Kuo L-R, Chang C-L, Hwu Y-K, Huang C-K, Lee S-Y, Chen K, Lin S-J, Huang J-D, Chen Y-Y. Biomaterials. 2010; 31:4104–4112. [PubMed: 20181393]

104. Wang H, Huff TB, Zweifel DA, He W, Low PS, Wei A, Cheng J-X. Proc. Natl. Acad. Sci. U. S. A. 2005; 102:15752–15756. [PubMed: 16239346]

105. Chen N-T, Tang K-C, Chung M-F, Cheng S-H, Huang C-M, Chu C-H, Chou P-T, Souris JS, Chen C-T, Mou C-Y, Lo L-W. Theranostics. 2014; 4:798–807. [PubMed: 24955141]

106. Zhao T, Yu K, Li L, Zhang T, Guan Z, Gao N, Yuan P, Li S, Yao SQ, Xu Q-H, Xu GQ. ACS Appl. Mater. Interfaces. 2014; 6:2700–2708. [PubMed: 24483257]

107. Ward WW, Cormier MJ. Photochem. Photobiol. 1978; 27:389–396.

108. Morin JG, Hastings JW. J. Cell Physiol. 1971; 77:313–318. [PubMed: 4397528]

109. Machleidt T, Woodroofe CC, Schwinn MK, Méndez J, Robers MB, Zimmerman K, Otto P, Daniels DL, Kirkland TA, Wood KV. ACS Chem. Bio. 2015; 10:1797–1804. [PubMed: 26006698]

110. Shimomura O, Musicki B, Kishi Y, Inouye S. Cell Calcium. 1993; 14:373–378. [PubMed: 8519061]

111. Xia Z, Rao J. Curr. Opin. Biotechnol. 2009; 20:37–44. [PubMed: 19216068]

112. Tsay JM, Trzoss M, Shi L, Kong X, Selke M, Jung ME, Weiss S. J. Am. Chem. Soc. 2007; 129:6865–6871. [PubMed: 17477530]

113. Yao H, Zhang Y, Xiao F, Xia Z, Rao J. Angew. Chem. Int. Ed. 2007; 46:4346–4349.

114. Hsu C-Y, Chen C-W, Yu H-P, Lin Y-F, Lai P-S. Biomaterials. 2013; 34:1204–1212. [PubMed: 23069718]

115. Kim YR, Kim S, Choi JW, Choi SY, Lee S-H, Kim H, Hahn SK, Koh GY, Yun SH. Theranostics. 2015; 5:805–817. [PubMed: 26000054]

116. Carpenter S, Fehr MJ, Kraus GA, Petrich JW. Proc. Natl. Acad. Sci. U. S. A. 1994; 91:12273–12277. [PubMed: 7991618]

117. Theodossiou T, Hothersall JS, Woods EA, Okkenhaug K, Jacobson J, MacRobert AJ. Cancer Res. 2003; 63:1818–1821. [PubMed: 12702568]

118. Schipper ML, Patel MR, Gambhir SS. Mol. Imaging Biol. 2006; 8:218–225. [PubMed: 16791748]

119. Boeckman HJ, Trego KS, Turchi JJ. Mol. Cancer Biol. 2005; 3:277–285.

120. Band IM, Kharitonov YI, Trzhaskovskaya MB. At. Data. Nucl. Data. 1979; 23:443–505.

121. Ahmad M, Pratx G, Bazalova M, Xing L. IEEE Access. 2014; 2:1051–1061.

122. Rogalski MM, Anker JN. Phys. Chem. Chem. Phys. 2012; 14:13469–13486. [PubMed: 22962667]

123. Ma L, Zou X, Chen W. J. Biomed. Nanotechnol. 2014; 10:1501–1508. [PubMed: 25016650]

124. Wang C, Volotskova O, Lu K, Ahmad M, Sun C, Xing L, Lin W. J. Am. Chem. Soc. 2014; 136:6171–6174. [PubMed: 24730683]

125. Osakada Y, Pratx G, Sun C, Sakamoto M, Ahmad M, Volotskova O, Ong Q, Teranishi T, Harada Y, Xing L, Cui B. Chem. Commun. 2014; 50:3549–3551.

126. Sun C, Pratx G, Carpenter CM, Liu H, Cheng Z, Gambhir SS, Xing L. Adv. Mater. 2011; 23:H195–H199. [PubMed: 21557339]

127. Chen H, Wang GD, Chuang Y-J, Zhen Z, Chen X, Biddinger P, Hao Z, Liu F, Shen B, Pan Z, Xie J. Nano Lett. 2015; 15:2249–2256. [PubMed: 25756781]

128. Yang W, Read PW, Mi J, Baisden JM, Reardon KA, Larner JM, Helmke BP, Sheng K. Int. J. Radiat. Oncol. Biol. Phys. 2008; 72:633–635. [PubMed: 19014777]

129. Naczynski DJ, Sun C, Türkcan S, Jenkins C, Koh AL, Ikeda D, Pratx G, Xing L. Nano Lett. 2015; 15:96–102. [PubMed: 25485705]

130. Kaš áková S, Giuliani A, Lacerda S, Pallier A, Mercère P, Tóth É, Réfrégiers M. Nano Res. 2015; 8:2373–2379.

131. Zou X, Yao M, Ma L, Hossu M, Han X, Juzenas P, Chen W. Nanomedicine. 2014; 9:2339–2351. [PubMed: 24471504]

132. Ma L, Zou X, Bui B, Chen W, Song KH, Solberg T. Appl. Phys. Lett. 2014; 105:013702.

133. Ma L, Chen W, Schatte G, Wang W, Joly AG, Huang Y, Sammynaiken R, Hossu M. J. Mater. Chem. C. 2014; 2:4239–4246.

134. Zhang C, Zhao K, Bu W, Ni D, Liu Y, Feng J, Shi J. Angew. Chem. Int. Ed. 2015; 54:1770–1774.

135. Clement S, Deng W, Camilleri E, Wilson BC, Goldys EM. Sci. Rep. 2016; 6:19954. [PubMed: 26818819]

136. Bulin A-L, Vasil'ev A, Belsky A, Amans D, Ledoux G, Dujardin C. Nanoscale. 2015; 7:5744–5751. [PubMed: 25746211]

137. Tanha K, Pashazadeh AM, Pogue BW. Biomed. Opt. Express. 2015; 6:3053–3065. [PubMed: 26309766]

138. Guo W, Sun X, Jacobson O, Yan X, Min K, Srivatsan A, Niu G, Kiesewetter DO, Chang J, Chen X. ACS Nano. 2015; 9:488–495. [PubMed: 25549258]

139. Sun X, Huang X, Guo J, Zhu W, Ding Y, Niu G, Wang A, Kiesewetter DO, Wang ZL, Sun S, Chen X. J. Am. Chem. Soc. 2014; 136:1706–1709. [PubMed: 24401138]

140. Ran C, Zhang Z, Hooker J, Moore A. Mol. Imaging Biol. 2012; 14:156–162. [PubMed: 21538154]

141. Kotagiri N, Sudlow GP, Akers WJ, Achilefu S. Nat. Nanotechnol. 2015; 10:370–379. [PubMed: 25751304]

142. Volotskova O, Sun C, Stafford JH, Koh AL, Ma X, Cheng Z, Cui B, Pratx G, Xing L. Small. 2015; 11:4002–4008. [PubMed: 25973916]

143. Hu Z, Qu Y, Wang K, Zhang X, Zha J, Song T, Bao C, Liu H, Wang Z, Wang J, Liu Z, Liu H, Tian J. Nat. Commun. 2015; 6:7560. [PubMed: 26123615]

144. Quail DF, Joyce JA. Nat. Med. 2013; 19:1423–1437. [PubMed: 24202395]

145. Li H, Fan X, Houghton J. J. Cell Biochem. 2007; 101:805–815. [PubMed: 17226777]

146. Wang H-W, Putt ME, Emanuele MJ, Shin DB, Glatstein E, Yodh AG, Busch TM. Cancer Res. 2004; 64:7553–7561. [PubMed: 15492282]

147. Moen I, Stuhr LEB. Target Oncol. 2012; 7:233–242. [PubMed: 23054400]

148. Wilson WR, Hay MP. Nat. Rev. Cancer. 2011; 11:393–410. [PubMed: 21606941]

149. Höckel M, Vaupel P. J. Natl. Cancer I. 2001; 93:266–276.

150. Maier A, Anegg U, Fell B, Rehak P, Ratzenhofer B, Tomaselli F, Sankin O, Pinter H, Smolle-Jüttner FM, Friehs GB. Laser. Surg. Med. 2000; 26:308–315.

151. Fuchs J, Thiele J. Free. Radical. Biol. Med. 1998; 24:835–847. [PubMed: 9586814]

152. Ding H, Yu H, Dong Y, Tian R, Huang G, Boothman DA, Sumer BD, Gao J. J. Controlled Release. 2011; 156:276–280.

153. Henderson BW, Fingar VH. Cancer Res. 1987; 47:3110–3114. [PubMed: 3581062]

154. Chapman JD, Stobbe CC, Arnfield MR, Santus R, Lee J, McPhee MS. Radiat. Res. 1991; 126:73–79. [PubMed: 1826959]

155. Krzykawska-Serda M, Dąbrowski JM, Arnaut LG, Szczygieł M, Urbańska K, Stochel G, Elas M. Free. Radical. Biol. Med. 2014; 73:239–251. [PubMed: 24835769]

156. Castano AP, Mroz P, Hamblin MR. Nat. Rev. Cancer. 2006; 6:535–545. [PubMed: 16794636]

157. Yang L, Wei Y, Xing D, Chen Q. Laser. Surg. Med. 2010; 42:671–679.

158. Singel DJ, Stamler JS. Annu. Rev. Physiol. 2004; 67:99–145.

159. Duan L, Yan X, Wang A, Jia Y, Li J. ACS Nano. 2012; 6:6897–6904. [PubMed: 22732258]

160. Li T, Jing X, Huang Y. Macromol. Biosci. 2011; 11:865–875. [PubMed: 21312333]

161. Modery-Pawlowski CL, Tian LL, Pan V, Sen Gupta A. Biomacromolecules. 2013; 14:939–948. [PubMed: 23452431]

162. Wang S, Yuan F, Chen K, Chen G, Tu K, Wang H, Wang L-Q. Biomacromolecules. 2015; 16:2693–2700. [PubMed: 26207413]

163. Luo Z, Zheng M, Zhao P, Chen Z, Siu F, Gong P, Gao G, Sheng Z, Zheng C, Ma Y, Cai L. Sci. Rep. 2016; 6:23393. [PubMed: 26987618]

164. Zhao P, Zheng M, Luo Z, Fan X, Sheng Z, Gong P, Chen Z, Zhang B, Ni D, Ma Y, Cai L. Adv. Healthc. Mater. 2016 DOI: 10.1002/adhm.201600121.

165. Tang W, Zhen Z, Wang M, Wang H, Chuang Y-J, Zhang W, Wang GD, Todd T, Cowger T, Chen H, Liu L, Li Z, Xie J. Adv. Funct. Mater. 2016; 26:1757–1768.

166. Spahn DR. Crit. Care. 1999; 3:R93–R97. [PubMed: 11094488]

167. Teicher BA, Herman TS, Holden SA, Liu S, Menon K. Radiat. Oncol. Invest. 1993; 1:14–19.

168. Spiess BD. J. Appl. Physiol. 2009; 106:1444–1452. [PubMed: 19179651]

169. Song G, Liang C, Yi X, Zhao Q, Cheng L, Yang K, Liu Z. Adv. Mater. 2016; 28:2716–2723. [PubMed: 26848553]

170. Castro CI, Briceno JC. Artif. Organs. 2010; 34:622–634. [PubMed: 20698841]

171. Lee H-Y, Kim H-W, Lee JH, Oh SH. Biomaterials. 2015; 53:583–591. [PubMed: 25890754]

172. Palumbo FS, Di Stefano M, Palumbo Piccionello A, Fiorica C, Pitarresi G, Pibiri I, Buscemi S, Giammona G. RSC Adv. 2014; 4:22894–22901.

173. Yao Y, Zhang M, Liu T, Zhou J, Gao Y, Wen Z, Guan J, Zhu J, Lin Z, He D. ACS Appl. Mater. Interfaces. 2015; 7:18369–18378. [PubMed: 26222132]

174. Teicher B, Rose C. Science. 1984; 223:934–936. [PubMed: 6695191]

175. Chin LS, Lim M, Hung TT, Marquis CP, Amal R. RSC Adv. 2014; 4:13052–13060.

176. Zhou Z, Zhang B, Zhang H, Huang X, Hu Y, Sun L, Wang X, Zhang J. Acta Pharmacol. Sin. 2009; 30:1577–1584. [PubMed: 19890365]

Author Manuscript

Author Manuscript

Author Manuscript

Author Manuscript

177. Huang C-C, Chia W-T, Chung M-F, Lin K-J, Hsiao C-W, Jin C, Lim W-H, Chen C-C, Sung H-W. J. Am. Chem. Soc. 2016; 138:5222–5225. [PubMed: 27075956]

178. Cheng H, Jiang C, Qiu X, Wang K, Huan W, Yuan A, Wu J, Hu Y. Nat. Commun. 2015; 6:8785. [PubMed: 26525216]

179. Donat RS, Roman K. Curr. Pharm. Design. 2005; 11:4099–4114.

180. Flaim SF. Artif. Cells Blood Substit. Immobil. Biotechnol. 1994; 22:1043–1054. [PubMed: 7849908]

181. Price M, Terlecky SR, Kessel D. Photochem. Photobiol. 2009; 85:1491–1496. [PubMed: 19659920]

182. Ho Y-S, Xiong Y, Ma W, Spector A, Ho DS. J. Biol. Chem. 2004; 279:32804–32812. [PubMed: 15178682]

183. Amo T, Atomi H, Imanaka T. J. Bacteriol. 2002; 184:3305–3312. [PubMed: 12029047]

184. Chen H, Tian J, He W, Guo Z. J. Am. Chem. Soc. 2015; 137:1539–1547. [PubMed: 25574812]

185. Zhang Y, Shen T-T, Kirillov AM, Liu W-S, Tang Y. Chem. Commun. :2016.

186. Zhu W, Dong Z, Fu T, Liu J, Chen Q, Li Y, Zhu R, Xu L, Liu Z. Adv. Funct. Mater. 2016 n/a-n/a.

187. Nitzan Y, Wexler HM, Finegold SM. Curr. Microbiol. 1994; 29:125–131. [PubMed: 7765091]

188. Howes PD, Rana S, Stevens MM. Chem. Soc. Rev. 2014; 43:3835–3853. [PubMed: 24323079]

189. Hu M, Chen J, Li Z-Y, Au L, Hartland GV, Li X, Marquez M, Xia Y. Chem. Soc. Rev. 2006; 35:1084–1094. [PubMed: 17057837]

190. Schuller JA, Barnard ES, Cai W, Jun YC, White JS, Brongersma ML. Nat. Mater. 2010; 9:193–204. [PubMed: 20168343]

191. Dreaden EC, Mackey MA, Huang X, Kang B, El-Sayed MA. Chem. Soc. Rev. 2011; 40:3391–3404. [PubMed: 21629885]

192. Yuan Q, Zhang Y, Chen T, Lu D, Zhao Z, Zhang X, Li Z, Yan C-H, Tan W. ACS Nano. 2012; 6:6337–6344. [PubMed: 22670595]

193. Mal NK, Fujiwara M, Tanaka Y. Nature. 2003; 421:350–353. [PubMed: 12540896]

194. Liu Y, Wang Z, Zhang H, Lang L, Ma Y, He Q, Lu N, Huang P, Liu Y, Song J, Liu Z, Gao S, Ma Q, Kiesewetter DO, Chen X. Nanoscale. 2016; 8:10553–10557. [PubMed: 27149392]

195. Asadirad AM, Erno Z, Branda NR. Chem. Commun. 2013; 49:5639–5641.

196. Baumes JM, Gassensmith JJ, Giblin J, Lee J-J, White AG, Culligan WJ, Leevy WM, Kuno M, Smith BD. Nature Chem. 2010; 2:1025–1030. [PubMed: 21107365]

197. McCusker JK. Acc. Chem. Res. 2003; 36:876–887. [PubMed: 14674779]

198. Kolemen S, Ozdemir T, Lee D, Kim GM, Karatas T, Yoon J, Akkaya EU. Angew. Chem. Int. Ed. 2016; 55:3606–3610.

199. Turan IS, Yildiz D, Turksoy A, Gunaydin G, Akkaya EU. Angew. Chem. Int. Ed. 2016; 55:2875–2878.

200. Benz S, Nötzli S, Siegel JS, Eberli D, Jessen HJ. J. Med. Chem. 2013; 56:10171–10182. [PubMed: 24299550]

201. Wells PNT. Phys. Med. Biol. 2006; 51:R83. [PubMed: 16790922]

202. Miller D, Smith N, Bailey M, Czarnota G, Hynynen K, Makin I, C. American Institute of Ultrasound in Medicine Bioeffects. J. Ultrasound Med. 2012; 31:623–634. [PubMed: 22441920]

203. Couture O, Foley J, Kassell NF, Larrat B, Aubry J-F. Transl. Cancer Res. 2014; 3:494–511.

204. Schoellhammer CM, Schroeder A, Maa R, Lauwers GY, Swiston A, Zervas M, Barman R, DiCiccio AM, Brugge WR, Anderson DG, Blankschtein D, Langer R, Traverso G. Sci. Trans. Med. 2015; 7:310ra168–310ra168.

205. Li W-P, Su C-H, Chang Y-C, Lin Y-J, Yeh C-S. ACS Nano. 2016; 10:2017–2027. [PubMed: 26720714]

206. You DG, Deepagan VG, Um W, Jeon S, Son S, Chang H, Yoon HI, Cho YW, Swierczewska M, Lee S, Pomper MG, Kwon IC, Kim K, Park JH. Sci. Rep. 2016; 6:23200. [PubMed: 26996446]

207. McCaughan B, Rouanet C, Fowley C, Nomikou N, McHale AP, McCarron PA, Callan JF. Bioorg. Med. Chem. Lett. 2011; 21:5750–5752. [PubMed: 21875807]

208. Verhille M, Couleaud P, Vanderess R, Brault D, Barberi-Heyob M, Frochot C. Curr. Med. Chem. 2010; 17:3925–3943. [PubMed: 20858211]

209. Huang P, Xu C, Lin J, Wang C, Wang XS, Zhang CL, Zhou XJ, Guo SW, Cui DX. Theranostics. 2011; 1:240–250. [PubMed: 21562631]

210. Jin CS, Cui L, Wang F, Chen J, Zheng G. Adv. Healthc. Mater. 2014; 3:1240–1249. [PubMed: 24464930]

211. Wang S, Huang P, Chen X. Adv. Mater. 2016 DOI: 10.1002/adma.201601498.

212. Zheng G, Chen J, Stefflova K, Jarvi M, Li H, Wilson BC. Proc. Natl. Acad. Sci. U. S. A. 2007; 104:8989–8994. [PubMed: 17502620]

213. Chen J, Stefflova K, Niedre MJ, Wilson BC, Chance B, Glickson JD, Zheng G. J. Am. Chem. Soc. 2004; 126:11450–11451. [PubMed: 15366886]

214. Ogilby PR. Chem. Soc. Rev. 2010; 39:3181–3209. [PubMed: 20571680]

215. Schweitzer C, Schmidt R. Chem. Rev. 2003; 103:1685–1758. [PubMed: 12744692]

216. McCarthy JR, Weissleder R. ChemMedChem. 2007; 2:360–365. [PubMed: 17245681]

217. Lovell JF, Chen J, Jarvi MT, Cao W-G, Allen AD, Liu Y, Tidwell TT, Wilson BC, Zheng G. J. Phys. Chem. B. 2009; 113:3203–3211. [PubMed: 19708269]

218. He C, Liu D, Lin W. Chem. Rev. 2015; 115:11079–11108. [PubMed: 26312730]

219. Park J, Feng D, Yuan S, Zhou H-C. Angew. Chem. Int. Ed. 2015; 54:430–435.

220. Lim C-K, Heo J, Shin S, Jeong K, Seo YH, Jang W-D, Park CR, Park SY, Kim S, Kwon IC. Cancer Lett. 2013; 334:176–187. [PubMed: 23017942]

221. Choi KY, Swierczewska M, Lee S, Chen XY. Theranostics. 2012; 2:156–178. [PubMed: 22400063]

222. Jang B, Choi Y. Theranostics. 2012; 2:190–197. [PubMed: 22375157]

223. Gatenby RA, Gillies RJ. Nat. Rev. Cancer. 2004; 4:891–899. [PubMed: 15516961]

224. Tannock IF, Rotin D. Cancer Res. 1989; 49:4373–4384. [PubMed: 2545340]

225. Estrella V, Chen T, Lloyd M, Wojtkowiak J, Cornnell HH, Ibrahim-Hashim A, Bailey K, Balagurunathan Y, Rothberg JM, Sloane BF, Johnson J, Gatenby RA, Gillies RJ. Cancer Res. 2013; 73:1524–1535. [PubMed: 23288510]

226. Doria F, Folini M, Grande V, Cimino-Reale G, Zaffaroni N, Freccero M. Org. Biomol. Chem. 2015; 13:570–576. [PubMed: 25380512]

227. Wang Y, Zhou K, Huang G, Hensley C, Huang X, Ma X, Zhao T, Sumer BD, DeBerardinis RJ, Gao J. Nat. Mater. 2014; 13:204–212. [PubMed: 24317187]

228. Mi P, Kokuryo D, Cabral H, Wu H, Terada Y, Saga T, Aoki I, Nishiyama N, Kataoka K. Nat Nano. 2016; 11:724–730.

229. Albini A, Sporn MB. Nat. Rev. Cancer. 2007; 7:139–147. [PubMed: 17218951]

230. Lee ES, Gao Z, Bae YH. J. Controlled Release. 2008; 132:164–170.

231. Schmaljohann D. Adv. Drug Delivery Rev. 2006; 58:1655–1670.

232. Chen Q, Ke H, Dai Z, Liu Z. Biomaterials. 2015; 73:214–230. [PubMed: 26410788]

233. McDonnell SO, Hall MJ, Allen LT, Byrne A, Gallagher WM, O'Shea DF. J. Am. Chem. Soc. 2005; 127:16360–16361. [PubMed: 16305199]

234. Ozlem S, Akkaya EU. J. Am. Chem. Soc. 2009; 131:48–49. [PubMed: 19086786]

235. Jiang X-J, Lo P-C, Yeung S-L, Fong W-P, Ng DKP. Chem. Commun. 2010; 46:3188–3190.

236. Tian J, Zhou J, Shen Z, Ding L, Yu J-S, Ju H. Chem. Sci. 2015; 6:5969–5977.

237. Tian J, Ding L, Xu H-J, Shen Z, Ju H, Jia L, Bao L, Yu J-S. J. Am. Chem. Soc. 2013; 135:18850–18858. [PubMed: 24294991]

238. Liu G, Hu J, Zhang G, Liu S. Bioconjugate Chem. 2015; 26:1328–1338.

239. Nomoto T, Fukushima S, Kumagai M, Miyazaki K, Inoue A, Mi P, Maeda Y, Toh K, Matsumoto Y, Morimoto Y, Kishimura A, Nishiyama N, Kataoka K. Biomat. Sci. 2016; 4:826–838.

240. Wang N, Zhao Z, Lv Y, Fan H, Bai H, Meng H, Long Y, Fu T, Zhang X, Tan W. Nano Res. 2014; 7:1291–1301.

241. Tapeinos C, Pandit A. Adv. Mater. 2016 DOI: 10.1002/adma.201505376.

242. Lee SH, Gupta MK, Bang JB, Bae H, Sung H-J. Adv. Healthc. Mater. 2013; 2:908–915. [PubMed: 25136729]

243. Durantini AM, Greene LE, Lincoln R, Martínez SR, Cosa G. J. Am. Chem. Soc. 2016; 138:1215–1225. [PubMed: 26789198]

244. Kim H, Kim Y, Kim I-H, Kim K, Choi Y. Theranostics. 2014; 4:1–11.

245. Chen H, Niu G, Wu H, Chen X. Theranostics. 2016; 6:78–92. [PubMed: 26722375]

246. Desgrosellier JS, Cheresh DA. Nat. Rev. Cancer. 2010; 10:9–22. [PubMed: 20029421]

247. Vanneman M, Dranoff G. Nat. Rev. Cancer. 2012; 12:237–251. [PubMed: 22437869]

248. Fang X, Tan W. Acc. Chem. Res. 2010; 43:48–57. [PubMed: 19751057]

249. Cho EJ, Lee J-W, Ellington AD. Annu. Rev. Anal. Chem. 2009; 2:241–264.

250. Wu X, Chen J, Wu M, Zhao JX. Theranostics. 2015; 5:322–344. [PubMed: 25699094]

251. Xiao Z, Farokhzad OC. ACS Nano. 2012; 6:3670–3676. [PubMed: 22574989]

252. Shieh Y-A, Yang S-J, Wei M-F, Shieh M-J. ACS Nano. 2010; 4:1433–1442. [PubMed: 20166743]

253. Zhu G, Niu G, Chen X. Bioconjugate Chem. 2015; 26:2186–2197.

254. Zhu Z, Tang Z, Phillips JA, Yang R, Wang H, Tan W. J. Am. Chem. Soc. 2008; 130:10856–10857. [PubMed: 18661988]

255. Wang J, Zhu G, You M, Song E, Shukoor MI, Zhang K, Altman MB, Chen Y, Zhu Z, Huang CZ, Tan W. ACS Nano. 2012; 6:5070–5077. [PubMed: 22631052]

256. Han D, Zhu G, Wu C, Zhu Z, Chen T, Zhang X, Tan W. ACS Nano. 2013; 7:2312–2319. [PubMed: 23397942]

257. Stephanopoulos N, Tong GJ, Hsiao SC, Francis MB. ACS Nano. 2010; 4:6014–6020. [PubMed: 20863095]

258. Kruspe S, Meyer C, Hahn U. Mol. Ther. 2014; 3:143.

259. Lennarz S, Alich TC, Kelly T, Blind M, Beck H, Mayer G. Angew. Chem. Int. Ed. 2015; 54:5369–5373.

260. Ruff KM, Snyder TM, Liu DR. J. Am. Chem. Soc. 2010; 132:9453–9464. [PubMed: 20565094]

261. Salvati E, Doria F, Manoli F, D'Angelo C, Biroccio A, Freccero M, Manet I. Org. Biomol. Chem. 2016; 14:7238–7249. [PubMed: 27383473]

262. Doria F, Manet I, Grande V, Monti S, Freccero M. J. Org. Chem. 2013; 78:8065–8073. [PubMed: 23869544]

263. Dinçalp H, Kızılok , çli S. J. Fluoresc. 2014; 24:917–924. [PubMed: 24596056]

264. Yuan Q, Wu Y, Wang J, Lu D, Zhao Z, Liu T, Zhang X, Tan W. Angew. Chem. Int. Ed. 2013; 52:13965–13969.

265. Yu Z, Pan W, Li N, Tang B. Chem. Sci. 2016; 7:4237–4244.

266. Pan L, Liu J, Shi J. Adv. Funct. Mater. 2014; 24:7318–7327.

267. Huang H, Yu B, Zhang P, Huang J, Chen Y, Gasser G, Ji L, Chao H. Angew. Chem. Int. Ed. 2015; 54:14049–14052.

268. Han K, Lei Q, Wang S-B, Hu J-J, Qiu W-X, Zhu J-Y, Yin W-N, Luo X, Zhang X-Z. Adv. Funct. Mater. 2015; 25:2961–2971.

269. Lv W, Zhang Z, Zhang KY, Yang H, Liu S, Xu A, Guo S, Zhao Q, Huang W. Angew. Chem. Int. Ed. 2016; 55:9947–9951.

270. Rosenkranz AA, Jans DA, Sobolev AS. Immunol. Cell Biol. 2000; 78:452–464. [PubMed: 10947873]

271. Rajendran L, Knolker H-J, Simons K. Nat. Rev. Drug Discov. 2010; 9:29–42. [PubMed: 20043027]

272. Shu X, Lev-Ram V, Deerinck TJ, Qi Y, Ramko EB, Davidson MW, Jin Y, Ellisman MH, Tsien RY. PLoS Biol. 2011; 9:e1001041. [PubMed: 21483721]

273. Giepmans BNG, Adams SR, Ellisman MH, Tsien RY. Science. 2006; 312:217–224. [PubMed: 16614209]

274. Qi YB, Garren EJ, Shu X, Tsien RY, Jin Y. Proc. Natl. Acad. Sci. U. S. A. 2012; 109:7499–7504. [PubMed: 22532663]

275. Bulina ME, Chudakov DM, Britanova OV, Yanushevich YG, Staroverov DB, Chepurnykh TV, Merzlyak EM, Shkrob MA, Lukyanov S, Lukyanov KA. Nat. Biotech. 2006; 24:95–99.

276. Frommer WB, Davidson MW, Campbell RE. Chem. Soc. Rev. 2009; 38:2833–2841. [PubMed: 19771330]

277. Wojtovich AP, Foster TH. Redox Biology. 2014; 2:368–376. [PubMed: 24563855]

278. Takehara K, Tazawa H, Okada N, Hashimoto Y, Kikuchi S, Kuroda S, Kishimoto H, Shirakawa Y, Narii N, Mizuguchi H, Urata Y, Kagawa S, Fujiwara T. Mol. Cancer Ther. 2016; 15:199–208. [PubMed: 26625896]

279. Liao Z-X, Li Y-C, Lu H-M, Sung H-W. Biomaterials. 2014; 35:500–508. [PubMed: 24112805]

280. Ruiz-González R, Cortajarena AL, Mejias SH, Agut M, Nonell S, Flors C. J. Am. Chem. Soc. 2013; 135:9564–9567. [PubMed: 23781844]

281. Serebrovskaya EO, Edelweiss EF, Stremovskiy OA, Lukyanov KA, Chudakov DM, Deyev SM. Proc. Natl. Acad. Sci. U. S. A. 2009; 106:9221–9225. [PubMed: 19458251]

282. Takemoto K, Matsuda T, Sakai N, Fu D, Noda M, Uchiyama S, Kotera I, Arai Y, Horiuchi M, Fukui K, Ayabe T, Inagaki F, Suzuki H, Nagai T. Sci. Rep. 2013; 3:2629. [PubMed: 24043132]

283. Mironova KE, Proshkina GM, Ryabova AV, Stremovskiy OA, Lukyanov SA, Petrov RV, Deyev SM. Theranostics. 2013; 3:831–840. [PubMed: 24312153]

284. He J, Wang Y, Missinato MA, Onuoha E, Perkins LA, Watkins SC, St Croix CM, Tsang M, Bruchez MP. Nat. Meth. 2016; 13:263–268.

285. Deavall DG, Martin EA, Horner JM, Roberts R. J. Toxicol. 2012; 2012:13.

286. Renschler MF. Eur. J. Cancer. 2004; 40:1934–1940. [PubMed: 15315800]

287. Fu D, Calvo JA, Samson LD. Nat. Rev. Cancer. 2012; 12:104–120. [PubMed: 22237395]

288. Gupta SC, Hevia D, Patchva S, Park B, Koh W, Aggarwal BB. Antioxid. Redox Signal. 2011; 16:1295–1322.

289. Wang W, Adachi M, Zhang R, Zhou J, Zhu D. Pancreas. 2009; 38:e114–e123. [PubMed: 19342982]

290. Simunek T, Sterba M, Popelova O, Adamcova M, Hrdina R, Gersl V. Pharmacol. Rep. 2009; 61:154–171. [PubMed: 19307704]

291. Hasinoff BB, Davey JP. Biochem. Pharmacol. 1988; 37:3663–3669. [PubMed: 2845993]

292. Doroshow JH, Davies KJ. J. Biol. Chem. 1986; 261:3068–3074. [PubMed: 3005279]

293. Florea A-M, Büsselberg D. Cancers. 2011; 3:1351–1371. [PubMed: 24212665]

294. D'Autreaux B, Toledano MB. Nat. Rev. Mol. Cell Biol. 2007; 8:813–824. [PubMed: 17848967]

295. Rivera-Gil P, Jimenez De Aberasturi D, Wulf V, Pelaz B, Del Pino P, Zhao Y, De La Fuente JM, Ruiz De Larramendi I, Rojo T, Liang X-J, Parak WJ. Acc. Chem. Res. 2013; 46:743–749. [PubMed: 22786674]

296. Manke A, Wang L, Rojanasakul Y. BioMed Res. Inter. 2013; 2013:15.

297. Fu PP, Xia Q, Hwang H-M, Ray PC, Yu H. J. Food Drug Anal. 2014; 22:64–75. [PubMed: 24673904]

298. Ren L, Zhong W. Environ. Sci. Technol. 2010; 44:6954–6958. [PubMed: 20715868]

299. Musameh M, Wang J, Merkoci A, Lin Y. Electrochem. Commun. 2002; 4:743–746.

300. Yan Y, Zheng W, Su L, Mao L. Adv. Mater. 2006; 18:2639–2643.

301. Hsieh H-S, Jafvert CT. Carbon. 2015; 89:361–371.

302. Hsieh H-S, Wu R, Jafvert CT. Environ. Sci. Technol. 2014; 48:11330–11336. [PubMed: 25171301]

303. Huang P, Lin J, Wang X, Wang Z, Zhang C, He M, Wang K, Chen F, Li Z, Shen G, Cui D, Chen X. Adv. Mater. 2012; 24:5104–5110. [PubMed: 22718562]

304. Lim SY, Shen W, Gao Z. Chem. Soc. Rev. 2015; 44:362–381. [PubMed: 25316556]

305. Hola K, Zhang Y, Wang Y, Giannelis EP, Zboril R, Rogach AL. Nano Today. 2014; 9:590–603.

306. Hong G, Diao S, Antaris AL, Dai H. Chem. Rev. 2015; 115:10816–10906. [PubMed: 25997028]

307. Tang Y, Hu H, Zhang MG, Song J, Nie L, Wang S, Niu G, Huang P, Lu G, Chen X. Nanoscale. 2015; 7:6304–6310. [PubMed: 25782595]

308. Ge J, Lan M, Zhou B, Liu W, Guo L, Wang H, Jia Q, Niu G, Huang X, Zhou H, Meng X, Wang P, Lee C-S, Zhang W, Han X. Nat. Commun. 2014; 5

309. Dallas P, Rogers G, Reid B, Taylor RA, Shinohara H, Briggs GAD, Porfyrakis K. Chem. Phys. 2016; 465–466:28–39.

310. Carlson C, Hussain SM, Schrand AM, Braydich-Stolle LK, Hess KL, Jones RL, Schlager JJ. J. Phys. Chem. B. 2008; 112:13608–13619. [PubMed: 18831567]

311. Shi M, Kwon HS, Peng Z, Elder A, Yang H. ACS Nano. 2012; 6:2157–2164. [PubMed: 22390268]

312. Albanese A, Tang PS, Chan WCW. Annu. Rev. Biomed. Eng. 2012; 14:1–16. [PubMed: 22524388]

313. Zhang C, Bu W, Ni D, Zhang S, Li Q, Yao Z, Zhang J, Yao H, Wang Z, Shi J. Angew. Chem. Int. Ed. 2016; 55:2101–2106.

314. Lemire JA, Harrison JJ, Turner RJ. Nat. Rev. Micro. 2013; 11:371–384.

315. Shi J. Nanomedicine. 2016; 11:1189–1191. [PubMed: 27080928]

316. de Gracia Lux C, Joshi-Barr S, Nguyen T, Mahmoud E, Schopf E, Fomina N, Almutairi A. J. Am. Chem. Soc. 2012; 134:15758–15764. [PubMed: 22946840]

317. Zhang Y, Yin Q, Yin L, Ma L, Tang L, Cheng J. Angew. Chem. Int. Ed. 2013; 52:6435–6439.

318. Han Y-F, Phonthammachai N, Ramesh K, Zhong Z, White T. Environ. Sci. Technol. 2008; 42:908–912. [PubMed: 18323121]

319. Navalon S, de Miguel M, Martin R, Alvaro M, Garcia H. J. Am. Chem. Soc. 2011; 133:2218–2226. [PubMed: 21280633]

320. Yang, X.-j.; Xu, X.-m.; Xu, J.; Han, Y.-f. J. Am. Chem. Soc. 2013; 135:16058–16061. [PubMed: 24124647]

321. Chen X, Ma W, Li J, Wang Z, Chen C, Ji H, Zhao J. J. Phys. Chem. C. 2011; 115:4089–4095.

322. Chen J, Zhang W, Zhang M, Guo Z, Wang H, He M, Xu P, Zhou J, Liu Z, Chen Q. Nanoscale. 2015; 7:12542–12551. [PubMed: 26140326]

323. Costas M, Mehn MP, Jensen MP, Que L. Chem. Rev. 2004; 104:939–986. [PubMed: 14871146]

324. Miyamoto S, Martinez GR, Medeiros MHG, Di Mascio P. J. Photochem. Photobiol. B. 2014; 139:24–33. [PubMed: 24954800]

325. Adam W, Kazakov DV, Kazakov VP. Chem. Rev. 2005; 105:3371–3387. [PubMed: 16159156]

326. Chen G, Roy I, Yang C, Prasad PN. Chem. Rev. 2016; 116:2826–2885. [PubMed: 26799741]

327. Min Y, Caster JM, Eblan MJ, Wang AZ. Chem. Rev. 2015; 115:11147–11190. [PubMed: 26088284]

328. Bechet D, Couleaud P, Frochot C, Viriot M-L, Guillemin F, Barberi-Heyob M. Trends Biotechnol. 2008; 26:612–621. [PubMed: 18804298]

329. He X, Aker GW, Huang M-J, Watts DJ, Hwang H-M. Curr. Top. Med. Chem. 2015; 15:1887–1900. [PubMed: 25961519]
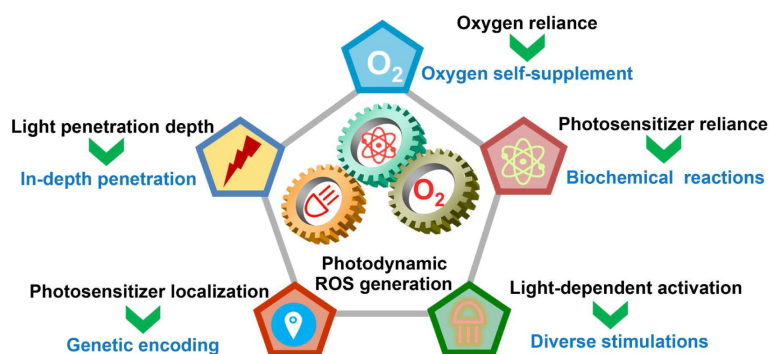
Fig. 1.
Schematic illustration of the mechanism of ROS generation through a typical photodynamic procedure. However, traditional photodynamic procedure encounters several challenges at difference levels (in black) blocking the broad applications of PDT. The overall contents are provided to summarize the advanced strategies to solve these problems through photodynamic and/or non-photodynamic procedures while highlighting the generation of ROS for cancer therapy.
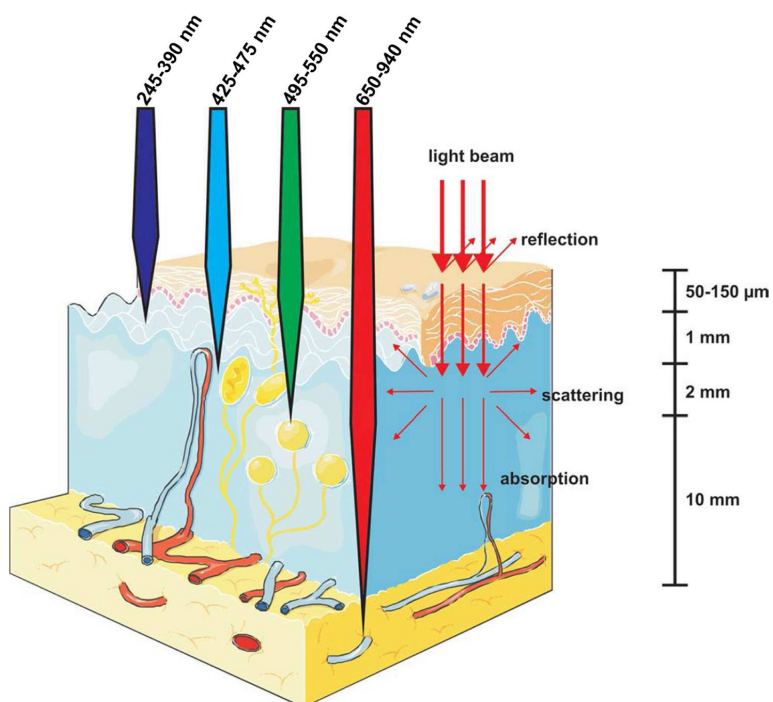
Fig. 2.
Light penetration through the tissues. The penetration depth of a typical light is dominated by the rates of absorption, scattering, transmission and reflection by tissue itself, which vary with different wavelengths. Adapted with permission from ref. 31. Copyright 2011, American Cancer Society.
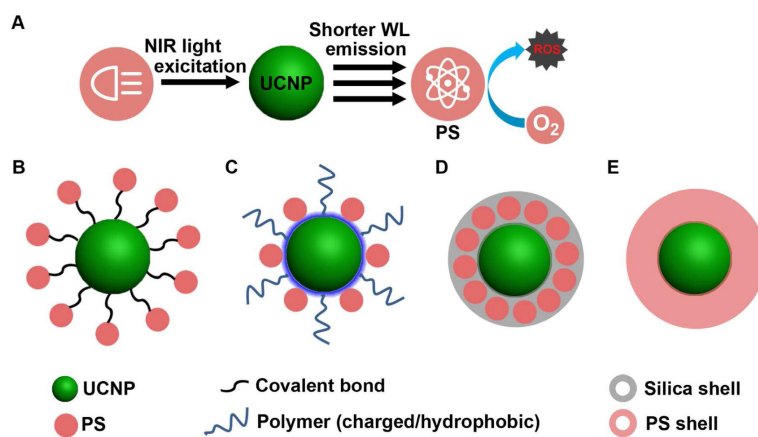
Fig. 3.
(A) NIR light harvesting by UCNP for photosensitizing PS and ROS generation. (B-E) Strategies for integrating UCNP and PS for PDT study including covalent binding (B), physical attachment through hydrophobic-hydrophobic interaction or electron static interaction (C), silica shell embedding (D), and direct PS coating (E).
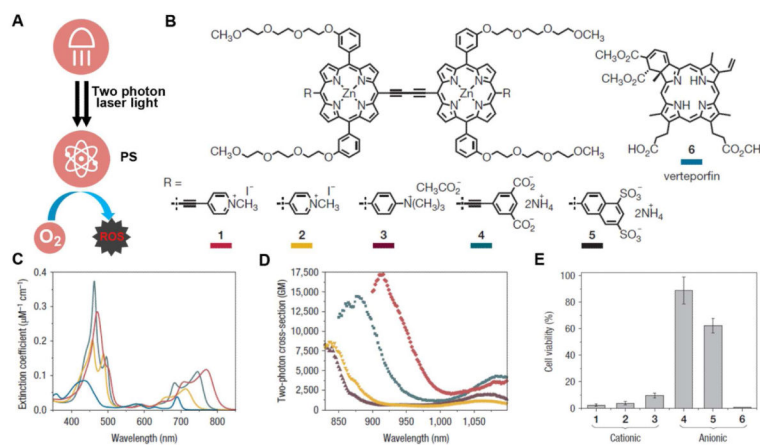
Fig. 4.
(A) Scheme of two-photon activation of PS for ROS generation. (B) Structures and absorption spectra of conjugated porphyrin dimers 1-5, and the clinically used photosensitizer verteporfin, 6. (C) One-photon absorption spectra of 1, 2, 4 and 6. (D) Two-photon absorption spectra of 1-4. All spectra were recorded in dimethylformamide (DMF) with 1% pyridine. (E) *In vitro* photodynamic therapy of porphyrin dimers 1-5, compared to verteporfin, 6. Reprinted with permission from ref. 96. Copyright 2008, Nature Publishing Group.
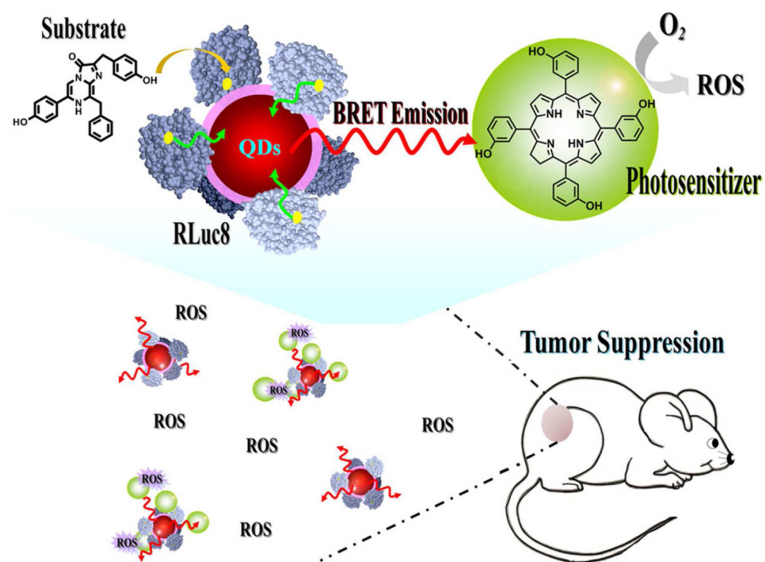
Fig. 5.
Schematic representation of RLuc8-immobilized QDs-655 for BRET-based PDT. Reprinted with permission from ref. 114. Copyright 2012, Elsevier Ltd.
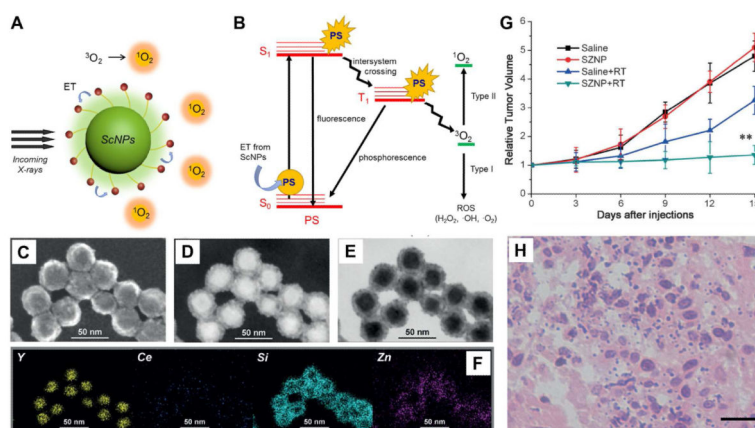
Fig. 6.

(A) Scintillating nanoparticles (ScNPs) act as an X-ray transducer to generate $^1O_2$ through the electron transfer process. (B) Diagram of the PDT mechanism that occurs when energy is transferred from ScNPs to activate the PS. (C-F) Scanning transmission electron microscope (STEM) image and corresponding element mapping (for Y, Ce, Si, and Zn) of ScNPs. (G, H) *In vivo* ionizing-radiation-induced ScNPs-mediated synchronous radiotherapy and PDT. Reprinted with permission from ref. 62. Copyright 2016, American Chemical Society. Reprinted with permission from ref. 134. Copyright 2015, John Wiley & Sons, Inc.
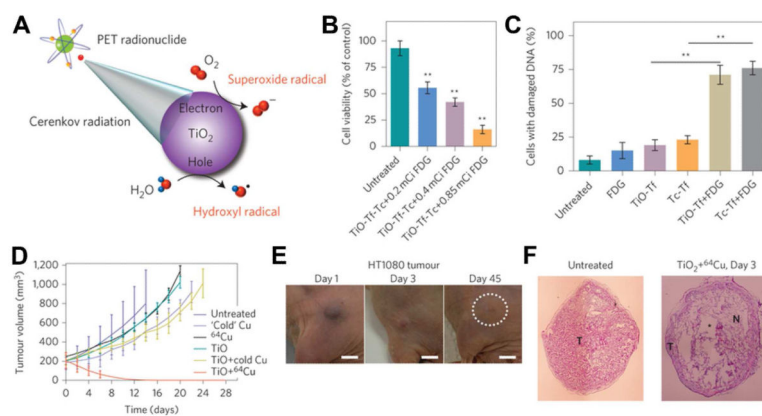
Fig. 7.
(A) Schematic of the CR-mediated excitation of TiO_2 nanoparticles to generate cytotoxic hydroxyl and superoxide radicals from water and dissolved oxygen, respectively, through electron-hole pair generation. CR is generated by PET radionuclides (not to scale). (B, C) Cell-viability and DNA damage by TiO_2 treatment. (D-F) *In vivo* CRIT through a one-time intra-tumoural administration shows significant shrinkage of tumour, and extensive necrotic centres and destruction of the tumour architecture from haematoxylin and eosin (H&E) slices. Reprinted with permission from ref. 141. Copyright 2015, Nature Publishing Group.
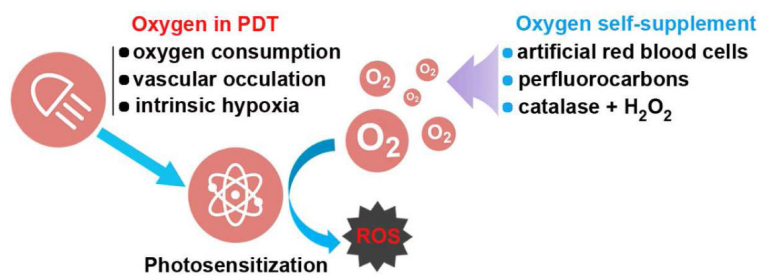
Fig. 8.
Scheme shows several situations of oxygen in PDT, indicating great importance for introducing oxygen self-supplied systems to confer efficient PDT outcomes.
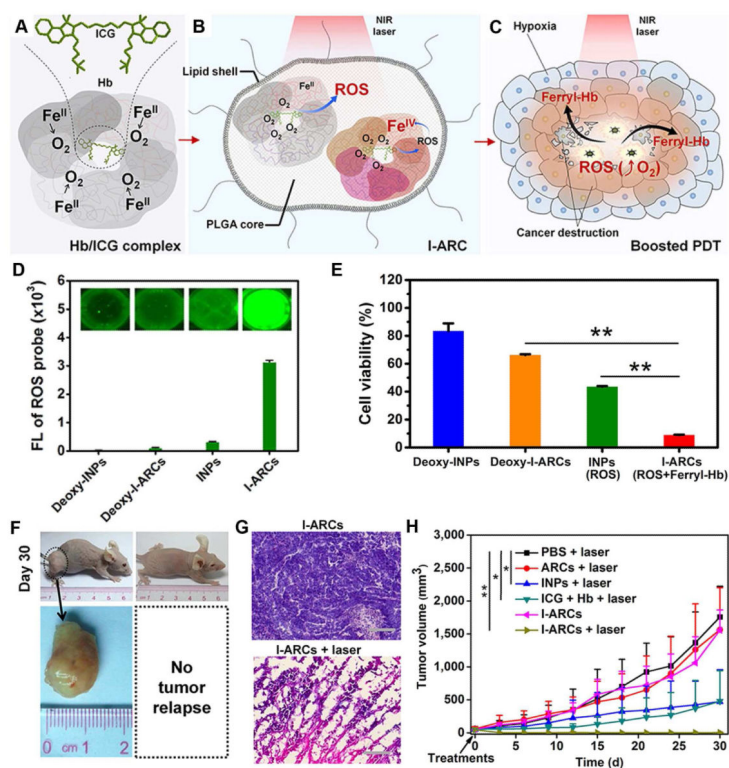
Fig. 9.
(A-C) Schematic illustration of cancer-boosted PDT based on ICG-loaded artificial red cells (I-ARCs) (D, E) ROS generation and ROS-mediated cell viability assay using I-ARCs. (F-G) *In vivo* anti-tumour evaluation of I-ARC-based PDT shows complete remission of MCF-7 tumours. Reprinted with permission from ref. 163. Copyright 2016, Nature Publishing Group.
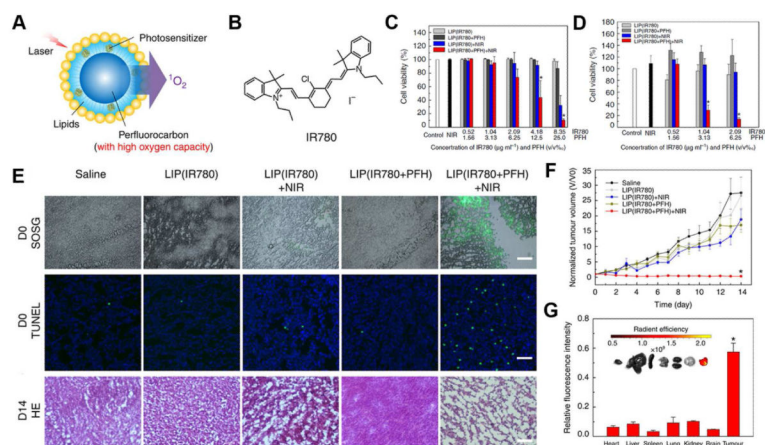
Fig. 10.
(A) Structure and design of the Oxy-PDT agent. (B) Structure of PS IR780. (C, D) Cell viability assay in CT-26 cells shows enhanced cytotoxicity by Oxy-PDT agents. (E-G) *In vivo* photodynamic therapy of Oxy-PDT by intra-tumoural injection in a subcutaneous tumour model, showing prominent $^1O_2$ generation and tumor growth inhibition. Reprinted with permission from ref. 178. Copyright 2015, Nature Publishing Group.
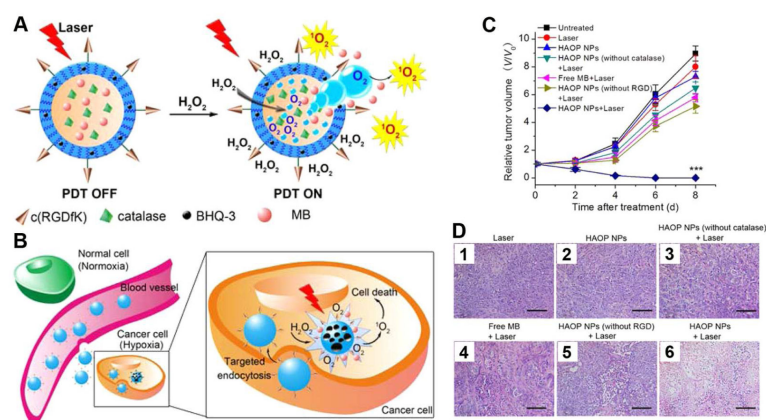
Fig. 11.
(A) Schematic illustration of mechanism of H_2O_2-controllable release of PS and O_2 to implement PDT and (B) HAOP NP for selective and efficient PDT against hypoxic tumor cell. (C) Change of relative tumor volume (V/V_0) and tumor slides by H&E staining upon different treatments. Scale bars: 100 μm. Reprinted with permission from ref. 184. Copyright 2015, American Chemical Society.
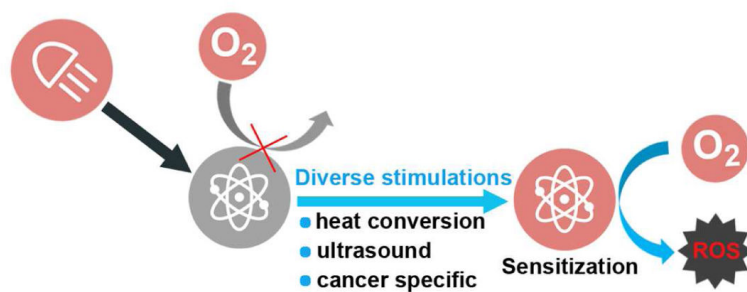
Fig. 12.
Scheme shows the ROS generation through diverse stimulations other than light activation of photosensitization, which could provide spatiotemporal control for ROS-based cancer therapy.
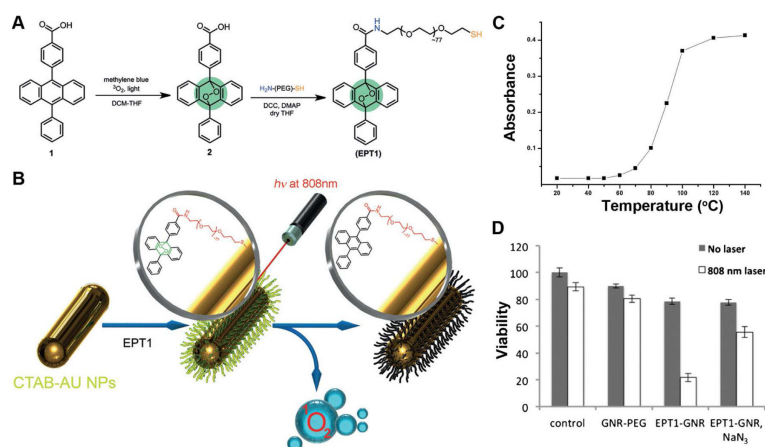
Fig. 13.
(A) Synthesis of the targeted anthracene endoperoxide derivative (EPT1) for gold nanorod functionalization. (B) PDT concept of photo-triggered thermal conversion and $^1O_2$ generation. (C) Absorbance at one of the anthracene peaks (404 nm) after heating EPT1 for 30 min at the indicated temperatures. (D) Viability assays of HeLa cells incubated with 10 pm of GNR-PEG or EPT1-GNR for 24 h, washed with DPBS, and irradiated with 808 nm laser (2.0 Wcm^{-2}, 10 min). Reprinted with permission from ref. 198. Copyright 2016, John Wiley & Sons, Inc.
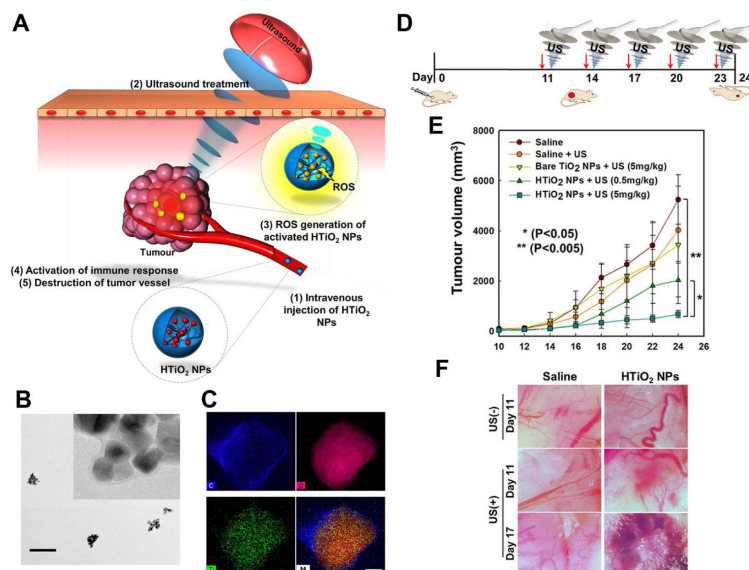
Fig. 14.
(A) Schematic illustration of sonodynamic therapy (SDT) using HTiO$_2$ NPs. (B, C) TEM EDS mapping and images of HTiO$_2$ NPs. Scale bar is 500 and 90 nm for B and C, respectively. (D) Treatment regimen of SDT. Red arrow represents injection time-points of HTiO$_2$ NPs. (F) Antitumour efficacy of HTiO$_2$ NPs in SCC7 tumour-bearing mice. (G) Bright-field images of tumour vasculature after SDT with US. Scale bar, 1000 μm. Reprinted with permission from ref. 206. Copyright 2016, Nature Publishing Group.
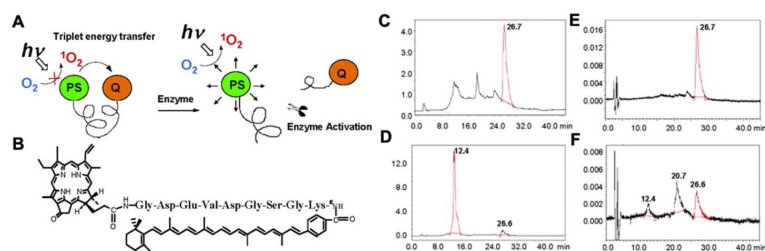
Fig. 15.
(A) Concept of $^1O_2$ quenching/scavenging and activation by an enzymatic cleavage of a caspase-3 substrate. (B) Structure of caspase-3 activatable Pyro-peptide-CAR (PPC) beacon. (C-F) HPLC chromatograms monitoring caspase-3 cleavage by (C,D) Pyro fluorescence and (E,F) CAR absorption: (C,E) PPC alone and (D,F) PPC + caspase-3. Reprinted with permission from ref. 213. Copyright 2004, American Chemical Society.
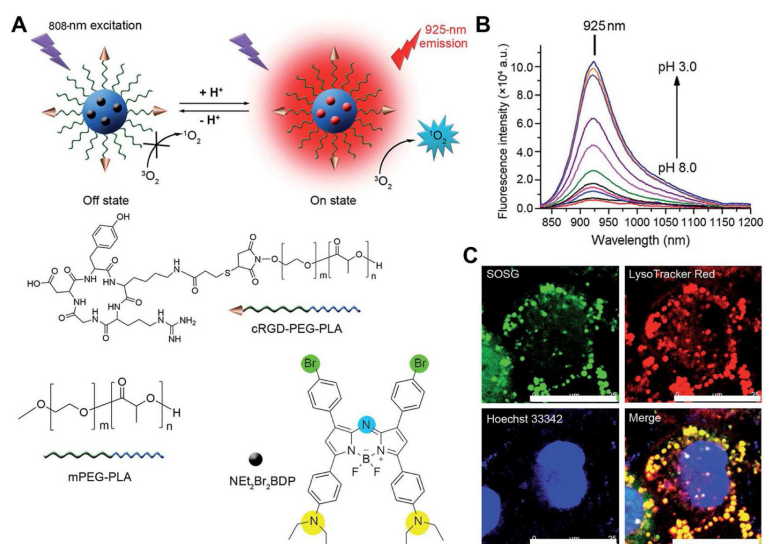
Fig. 16.
(A) Structures and pH-activatable generation of fluorescence and $^1O_2$ by cRGD-NEt$_2$Br$_2$BDP NP. (B) NIR fluorescence spectra of cRGD-NEt$_2$Br$_2$BDP NP at different pH. (C) Subcellular localization of $^1O_2$ generated during cRGD-NEt$_2$Br$_2$BDP NP-mediated PDT with singlet oxygen sensor green (SOSG), LysoTracker Red and Hoechst 33342 staining. Scale bars: 25 μm. Reprinted with permission from ref. 236. Copyright 2015, The Royal Society of Chemistry.
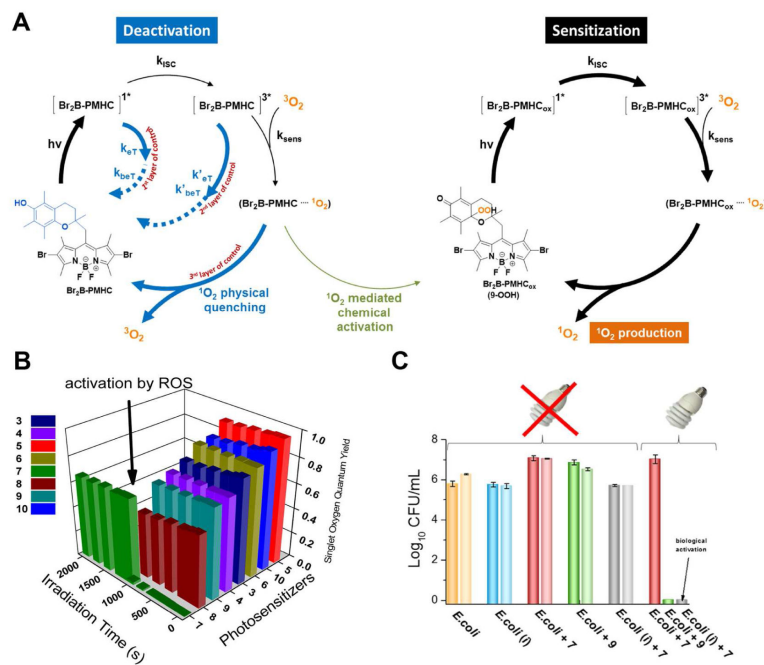
Fig. 17.

(A) Proposed mechanism for autocatalytic $^1O_2$ amplification. Following photoexcitation of Br$_2$B-PMHC, its singlet excited state rapidly deactivates via intra-molecular photo-induced electron transfer (PeT). The improbable occurrence of a chemical quenching pathway of $^1O_2$ by Br$_2$B−PMHC will yield an oxidized, active form, Br$_2$B−PMHCox that will sensitize additional $^1O_2$. (B) $^1O_2$ phosphorescence emission intensities (λ_{em} = 1270 nm) as a function of irradiation time for different PSs in air-equilibrated acetonitrile solutions. (C) Antibacterial photodynamic inactivation in *E. coli* ATCC 25922. *E. coli* dark controls (from left to right): control, incubated with 500 nM hydrogen peroxide. Reprinted with permission from ref. 243. Copyright 2016, American Chemical Society.
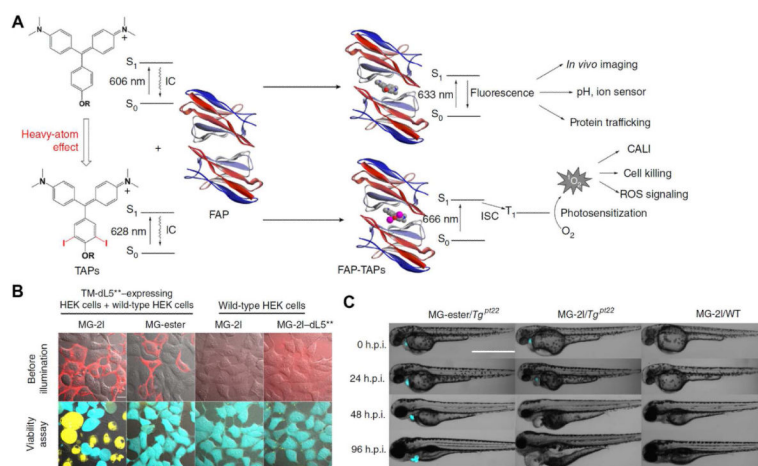
Fig. 18.
(A) Mechanism of ROS generation by FAP-TAPs. IC, internal conversion by molecule's free rotation; ISC, intersystem crossing. (B) Images of cells that were labeled with 400 nM of the indicated dye taken before laser illumination (top) by differential interference contrast (DIC) and fluorogen-FAP (red). Live cell (cyan) and dead cell (yellow) were assayed 30 min after illumination (bottom). Scale bar, 10 μm. (C) Merge of DIC and mCer3 fluorescence (cyan) showing phenotype development from 0 h p. i. to 96 h p. i. of larval zebrafish ($n = 20$ for each group). Scale bar: 1000 μm. Reprinted with permission from ref. 284. Copyright 2016, Nature Publishing Group.
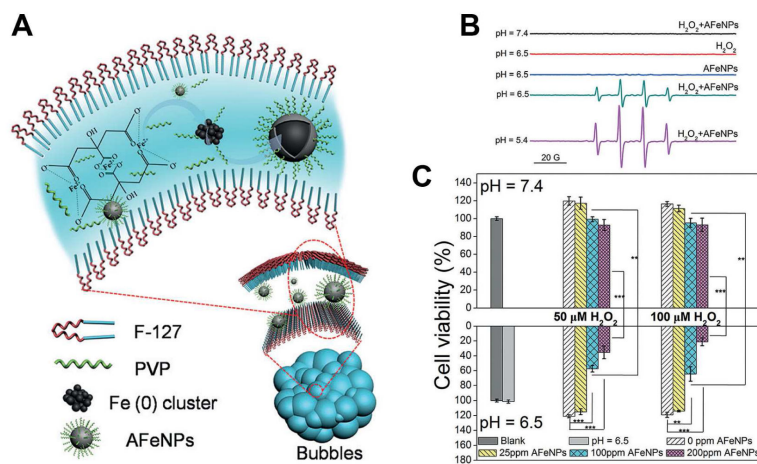
Fig. 19.
(A) Preparation of amorphous Fe^0 nanoparticles (AFeNPs). (B) Electron spin resonance (ESR) spectra of different reaction systems with 5, 5-Dimethyl-1-Pyrroline-N-Oxide (DMPO) as the spin trap. (C) Growth inhibitory effects of the AFeNPs on MCF-7 cells at pH 7.4 and 6.5 at various H_2O_2 concentrations (n = 6, mean ± s. d., **P<0.01, and ***P<0.001). Reprinted with permission from ref. 313. Copyright 2016, John Wiley & Sons, Inc.
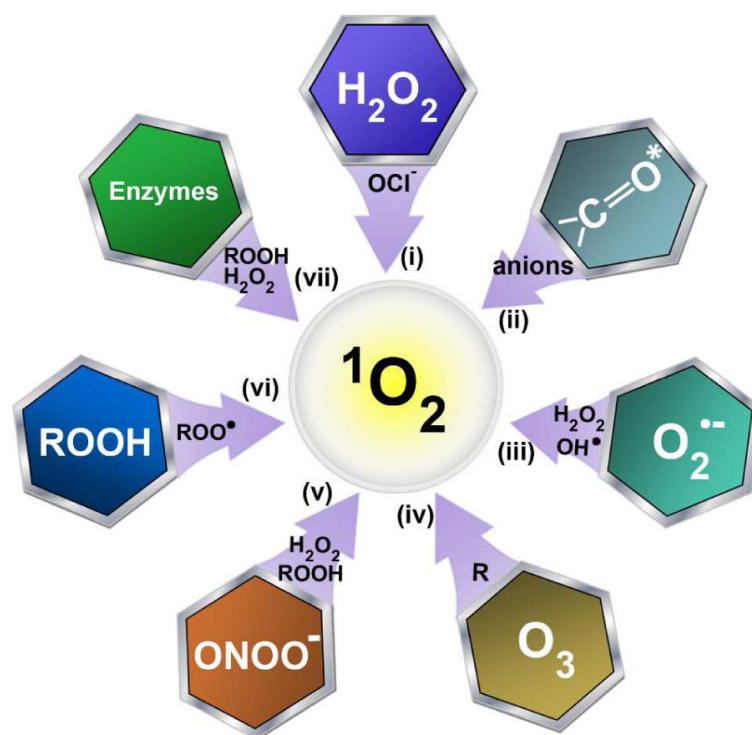
Fig. 20.
An overview of major biochemical reactions that are able to generate $^1O_2$. R indicates alkyl groups, enzymes include catalase and peroxidases. (i) H_2O_2 and hypochlorite (ClO^-) during phagocytosis; (ii) energy transfer reaction from excited carbonyl species; (iii) superoxide anion reactions with organic or inorganic substances; (iv) ozone reaction involving hydrotrioxide intermediates; (v) peroxynitrite reactions with hydroperoxides or hydrogen peroxides; (vi) decomposition of lipid hydroperoxides by reduction through Russell mechanism; (vii) enzymes (e.g., catalase, peroxidases)-involved metabolism.